Construction and Building Materials 345 (2022) 128323

Contents lists available at ScienceDirect

Construction and Building Materials

journal homepage: www.elsevier.com/locate/conbuildmat

The effect of biomolecules on enzyme-induced calcium carbonate precipitation in cementitious materials

Elvis Baffoe, Ali Ghahremaninezhad *

Department of Civil, Architectural and Environmental Engineering, University of Miami, Coral Gables, FL 33146, United States

ARTICLE INFO

Keywords:
EICP
Proteins
Healing

ABSTRACT

This study examined the effect of different proteins on the enzyme-induced calcium carbonate (EICP) processes in a cement environment. The ability of EICP to bind loosely packed ground hardened cement paste was evaluated as a model to shed light onto the crack surface binding processes of EICP. The adsorption of the proteins onto ground hardened cement paste and calcium carbonate ($CaCO_3$) was studied. The chemical and morphological characteristics of the microstructure were studied using Fourier transform infrared spectroscopy (FTIR), thermogravimetric analysis (TGA), scanning electron microscopy (SEM), and X-ray microcomputed tomography (micro-CT). The mechanical and water permeability of the samples were also investigated. It was shown that ettringite, $CaCO_3$, and calcium hydroxide (CH) were the main reaction products. Calcite was found to be the main polymorph of $CaCO_3$ in the samples. Samples modified with proteins were shown to result in a higher $CaCO_3$ content, compared to the control sample. The total porosity and pore size distribution were reduced in the sample modified with proteins, compared to the control sample. Overall, an increase in the tensile strength of the samples modified with proteins compared to the control sample was observed. Enhanced interfacial adhesion coupled with more densified microstructure are suggested to explain the improved tensile strength in the samples modified with proteins. Some proteins were shown to reduce the water permeability in the samples; lower porosity and smaller pore size distribution as well as the pore surface hydrophobization ability of these proteins contributed to reduced water permeability.

1. Introduction

Due to the relatively low tensile strength of concrete, cracking is a common phenomenon in concrete structures [1]. Cracks continuously develop in concrete due to mechanical and environmental conditions compromising concrete service life [2]. The self-healing concepts in cement-based materials have attracted significant interest over the past two decades [3–35]. Self-healing is generally categorized into autonomous and autogenous healing [36]. The autogenous healing is premised on further hydration of unreacted binder and carbonation of calcium hydroxide (CH) [37]. These binders can be ordinary Portland cement as well as other types, which are not fully hydrated in the initial stage of hydration, particularly, in low water/binder mixes [38]. However, such a mechanism is not effective in healing typical cracks in concrete because of the limited remaining potential and difficulties in optimizing the performance [38,39].

Researchers have investigated several methods to promote the autogenous healing effect. These include limiting crack widths by introducing fiber reinforcements in engineered cementitious composites (ECC) [5-8,30,31,33-35], supplying water for continued chemical reactions through use of superabsorbent polymers [9-11] or saturated lightweight aggregates [40], improving hydration and crystallization using mineral and chemical admixtures [12-14,16-18], and using polymer modified concrete (PMC) to extend the healing effect [41,42]. In the autonomous healing, healing materials are impregnated into a medium such as hydrogels, microcapsules, porous aggregates, or biochars, and mixed with the concrete [29,37,43-45]. The impregnated materials are released into the cracked zone when the impregnating medium ruptures or due to chemical triggers such as a change in pH of the cementitious environment [46]. Upon their release, they react with either the cementitious matrix, chemicals in the surrounding cementitious environment or other impregnated materials to heal and seal the crack surface [43,47]. In some instances, the healing material is directly mixed with the concrete for autonomous healing to occur [29,48]. Among the currently investigated self-healing strategies, the microbial-based strategy [1,49-51] and enzyme-based strategies [52] for self-healing

* Corresponding author.
E-mail address: a.ghahremani@miami.edu (A. Ghahremaninezhad).

https://doi.org/10.1016/j.conbuildmat.2022.128323
Received 7 March 2022; Received in revised form 29 June 2022; Accepted 30 June 2022
Available online 7 July 2022

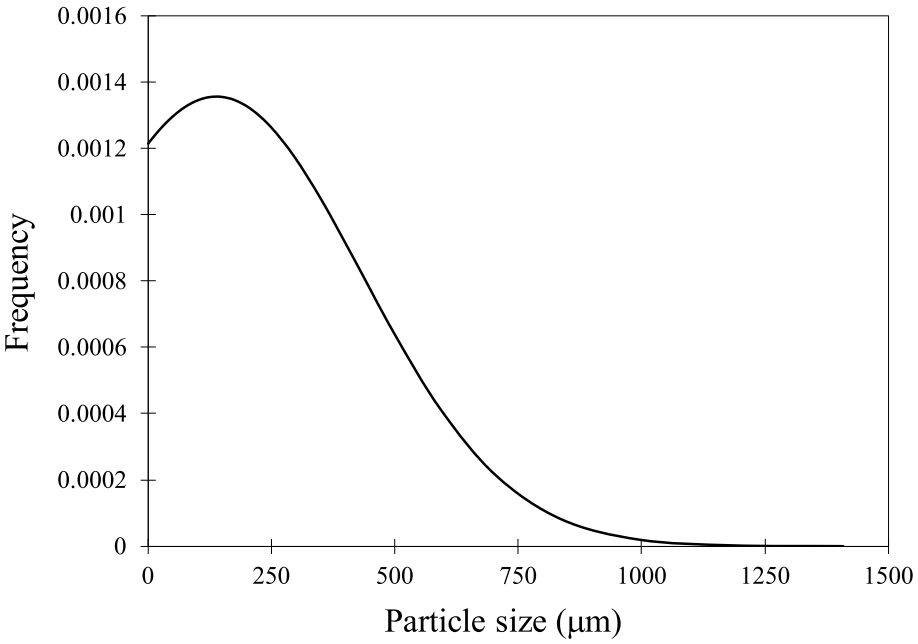

Fig. 1. Particle size distribution of the ground hardened cement.

concrete cracks are an emerging field. These techniques rely on the microbes or enzymes to precipitate calcium carbonate ($CaCO_3$). Microbial-induced carbonate precipitation (MICP) relies on the biomineralization capability of bacteria to produce the self-healing agent under suitable environmental conditions [53]. Unlike MICP, which relies on bacteria to generate urease enzyme, the enzyme-induced carbonate precipitation (EICP) depends on plant derived urease to catalyze the necessary reactions that precipitate $CaCO_3$ [52]. Despite the wide application of the MICP technique on sand consolidation, a few limitations of this method has been reported. For instance, Ahenkorah et al. [54] reported that for the same content of $CaCO_3$, the tensile strength of EICP-treated sand is markedly higher compared to the MICP-treated sand. The complexities associated with the MICP process such as the optimum conditions (temperature, oxygen, pH level) needed for specific bacteria growth may be daunting and not readily available [55,56]. In addition, the relative smaller size of the urease enzymes (~12 nm), as compared to the size of the microbes (typically ranging between 300 nm and 500 nm), allows EICP to be utilized in finer pore spaces [57]. The application of EICP has been explored in sand consolidation [54,58-62], a few on surface crack healing in mortars [52], and as a plugging material in reservoirs [63].

Proteins are the fundamental building blocks of impressive display of biomaterials involved in critical functions of life [64]. In the last 30 years, several proteins that regulate the biomineralization processes, including promotion of crystal formation [65-67], matrix-assisted orientation of crystal [68], growth inhibition by face-selective surface adsorption [69,70], and control of the crystal phase [69] have been isolated and analyzed. It has been shown in a recent study [71] that use of proteins extracted from nacre improves the MICP in sand biocementation.

Inspired by the intricate role of biomolecules in affecting the microstructure and properties of natural composites, this research seeks to investigate the influence of proteins on the EICP processes in a cement environment and to reveal the potential effect of proteins on the self-healing of cementitious materials utilizing EICP. Interestingly, some of the applications of EICP in sand consolidation and the surface crack healing of concrete have had proteins as part of the formulation [63,72-74]. For instance, Almajed et al. [72] investigated the effect of non-fat milk dairy powder (NFMP) on the soil strengthening and observed an improved soil strengthening, but with a low $CaCO_3$ content. They attributed this outcome to the precipitation of calcite at contact points between the particles due to the non-fat milk diary powder. Larsen et al. [63] applied EICP which has been modified with some proteins on fracture plugging in chalk reservoir. According to their findings, there was a ten-fold increase in $CaCO_3$ precipitation. They attributed this to the protection of the urease by other proteins stabilizing the urease against the environmental changes. Zulfikar et al. [73] utilized soybean protein to augment crack healing in concrete using EICP and observed a reduction in concrete permeability compared to the control samples. Ihsani and Putra [74] used milk as a catalyst for EICP healing in cracked concrete and observed an improved concrete permeability and concrete strength. They attributed this outcome to the possible influence of bacteria present in the milk. Pretreatment using concentrated protein solutions such as bovine serum albumin and milk have also been used to improve urease enzyme effectiveness with respect to precipitation efficiency [75,76]. These and many other studies have demonstrated the effectiveness and influence proteins have on soil strengthening and crack healing when EICP or any other healing material is involved. In spite of the afore-mentioned studies, the mechanisms underlying the effect of proteins on the EICP processes in a cement environment is not understood and lacking in the literature. Thus, in order to address this shortcoming, this paper aims to investigate the influence of five proteins with different characteristics on the EICP processes in a cement environment. The cement environment consisted of fine ground hardened cement paste. The ability of EICP to bind loosely packed ground hardened cement paste was studied as a model to provide insights into the crack surface binding processes of EICP. Use of ground hardened cement paste was motivated by increased surface area and as a result, higher interaction between the proteins, EICP, and ground hardened cement paste. This avoided some of the difficulty associated with extracting healing material in the interface between cement paste surfaces for chemical and morphological characterization. Techniques such as dynamic light scattering (DLS) and electrophoretic light scattering (ELS) were employed to study the size and charge of the proteins, respectively. Ultraviolet–visible (UV–Vis) spectrophotometry was utilized to study the adsorption isotherm of the proteins on the ground hardened cement paste and ($CaCO_3$). X-ray micro-computed tomography (micro-CT) and scanning electron microscopy (SEM) were used to evaluate the internal microstructure of the samples. Fourier transform infrared spectroscopy (FTIR) and thermogravimetric analysis (TGA) were adopted to study the

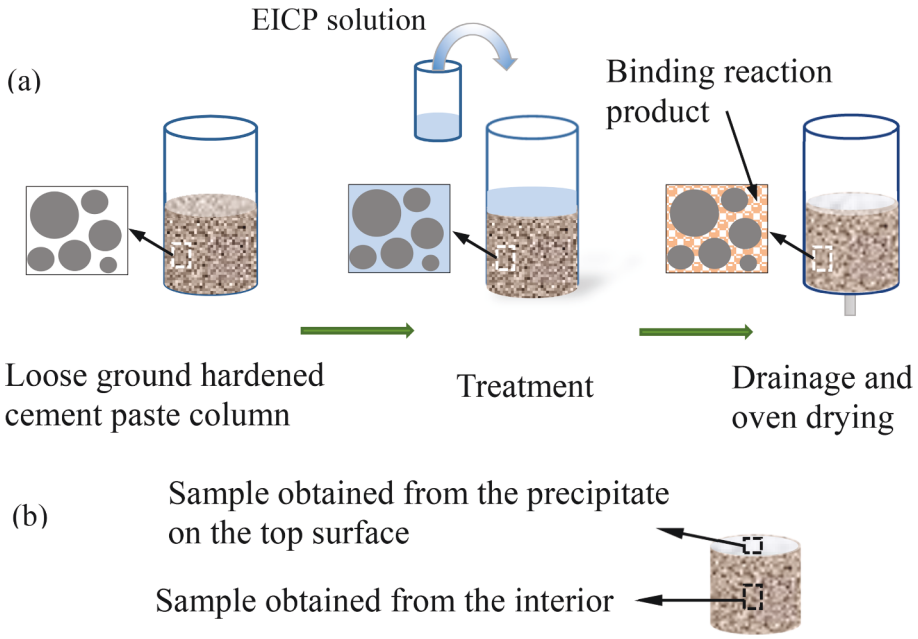

Fig. 2. Schematics illustrating (a) the treatment of the ground hardened cement paste with EICP and (b) samples used in the chemical and microscopic characterization experiments.

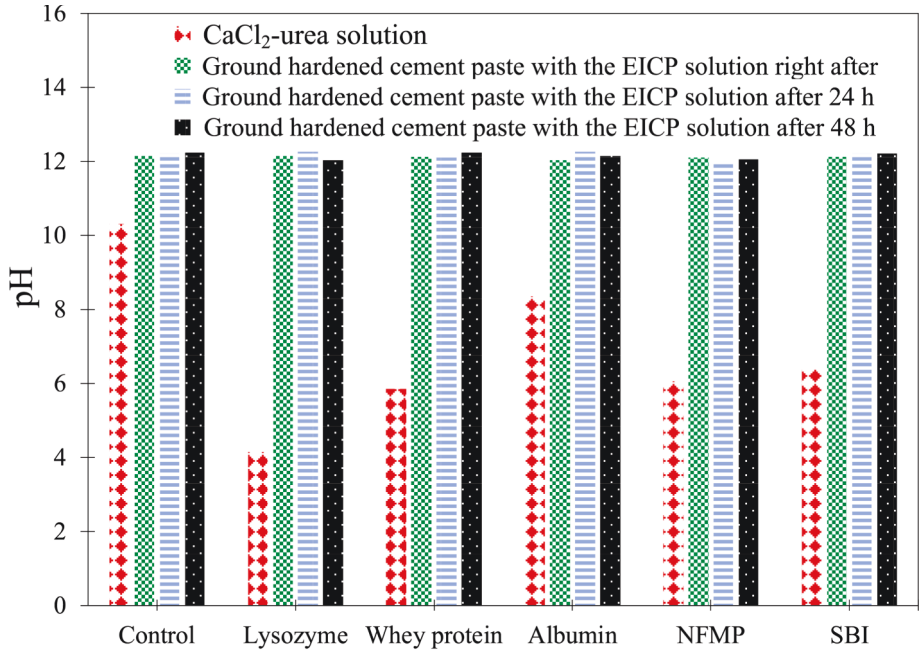

Fig. 3. pH of the ground hardened cement paste treated with the EICP solutions containing different proteins at different times. pH of the $CaCl_2$-urea solution with and without proteins is also included.

chemical characteristics of the healing product. Mechanical and permeability tests were conducted to examine the healing process in the samples.

2. Experiments

2.1. Materials

2.1.1. Proteins

Proteins in this study were purchased from commercial vendors and used as received. The proteins consisted of whey protein concentrate, lysozyme, non-fat milk powder (NFMP), serum-derived bovine immunoglobulin protein isolate (SBI), and albumin. These proteins have been investigated extensively for various applications including their applicability as foaming agents in food [77], biomineralization of $CaCO_3$ [78,79], and for sand consolidation [72]. Lysozyme is a globular protein extracted from egg white [80]. According to the literature [81], NFMP is made by removing moisture from non-fat milk, and contains 34–36% protein on dry mass. Casein protein constitutes a major portion of the milk proteins [81]. Whey protein concentrate is a by-product of the cheese making process and comprises 4 main classes of globular proteins, namely, bovine β-lactoglobulin, bovine α-lactalbumin, bovine serum albumin and immunoglobulins with bovine β-lactoglobulin constituting 50% [82]. The albumin used consists of ovalbumin which

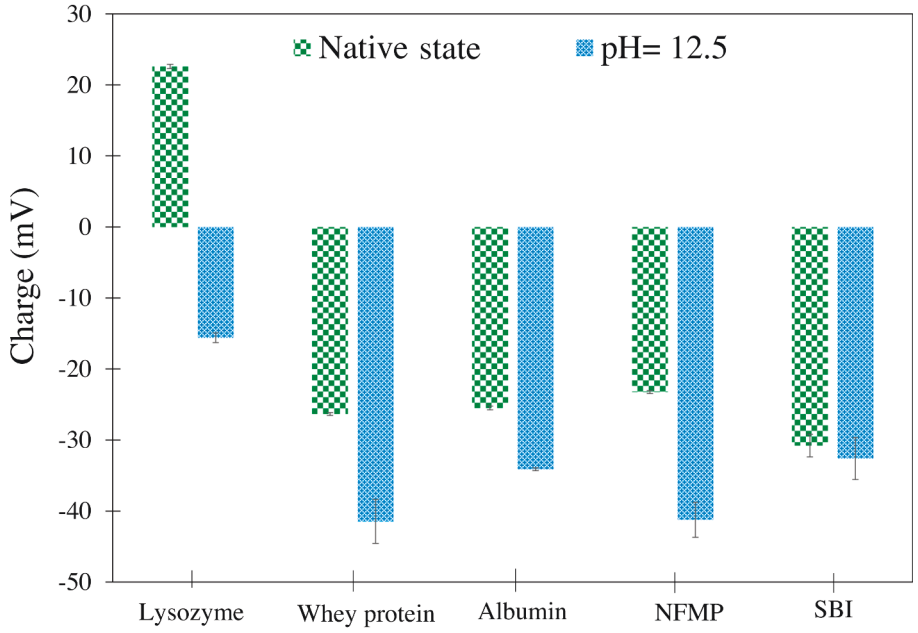

Fig. 4. Zeta potential of proteins in the native state and at the pH level of 12.5.

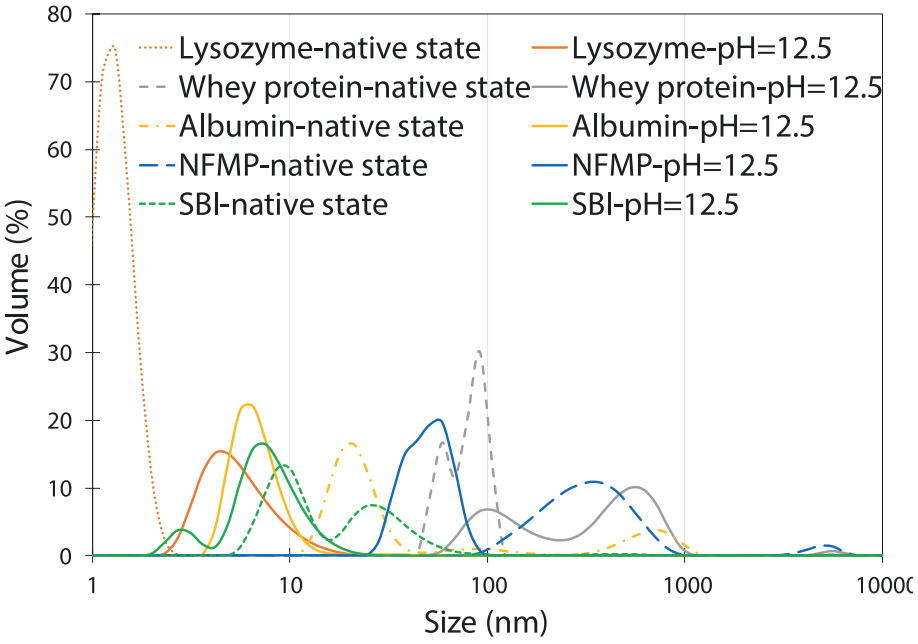

Fig. 5. Hydrodynamic size distribution by volume of the proteins at native state and at pH level of 12.5.

constitutes about 54% to 58% by weight of the egg white protein [83]. SBI is made up of about 90% protein and is prepared by separating edible grade bovine plasma into different fragments [84]. The commercial availability of these proteins at the scale needed for this study was a factor in their selection. It should be emphasized that due to a large amount of the proteins needed in the experiments, the procurement of these proteins in very high purity was cost prohibitive. It is expected that the proteins had impurities to a small extent.

2.1.2. Ground hardened cement paste

Cement paste with a water to cement ratio, w/c, of 0.4 was cast and cured for 28 days. After the 28-day curing, the paste was ground with the aid of a blender and passed through the Sieve #16. Fig. 1 illustrates the particle size distribution of the ground hardened cement paste as analyzed by the Microtrac S3500 Particle Analyzer. The average particle size of the ground hardened cement paste was 138 μm. To prepare the samples for the permeability and tensile strength tests, the ground hardened cement paste was cast into cylindrical molds of height 30 mm and diameter 40 mm and covered to avoid evaporation. The cylindrical molds were lined with a thin plastic sheet for the easy removal of the samples.

2.1.3. Calcium carbonate

$CaCO_3$ was prepared in the form of a powder to study the adsorption of the proteins onto $CaCO_3$. $CaCO_3$ was synthesized using the direct precipitation method by reacting calcium chloride ($CaCl_2$) and sodium

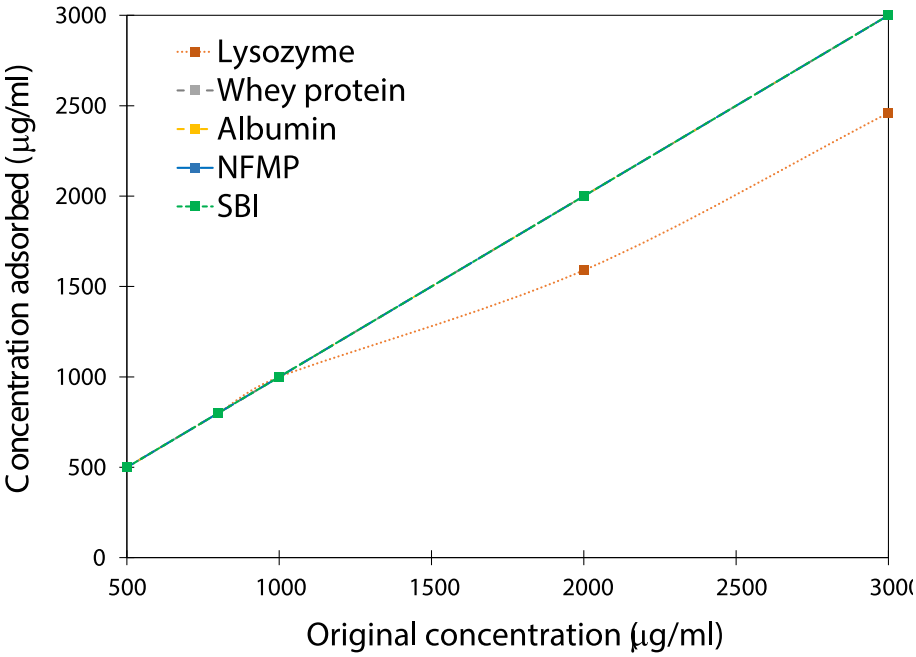

Fig. 6. Adsorption isotherm of proteins on ground hardened cement paste.

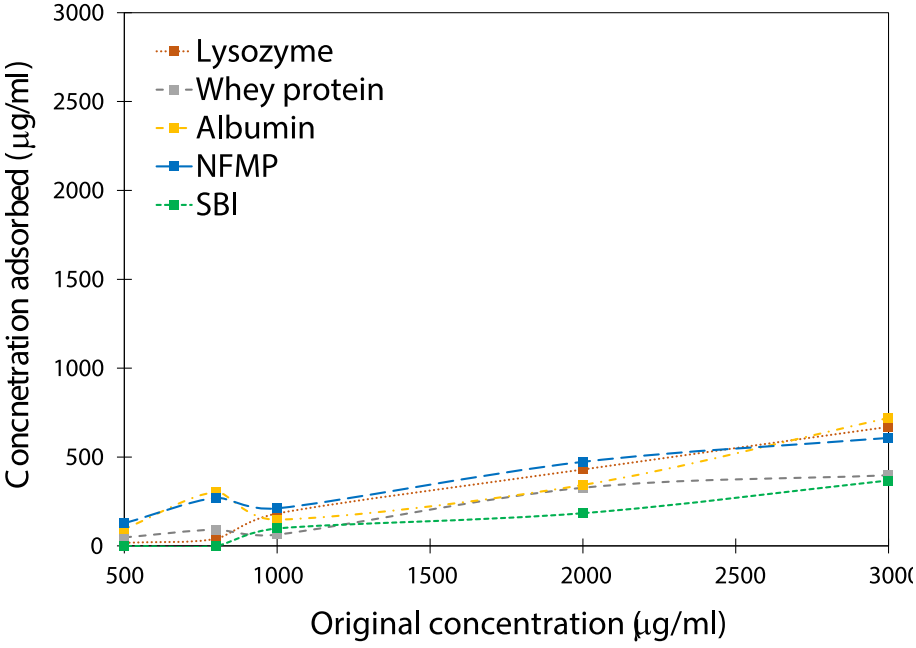

Fig. 7. Adsorption isotherm of proteins on $CaCO_3$ in the pore solution.

carbonate (Na_2CO_3) in an aqueous solution. The control crystallization solution was prepared by mixing equal volumes (200 mL) of 1.5 M equimolar concentration of $CaCl_2$ and Na_2CO_3, respectively, at pH level of 12.5. The precipitate was filtrated using a micro membrane filter with a 0.45 µm pore diameter under a negative pressure. The precipitate was washed with deionized water (DI) and acetone, and oven-dried at 50 °C under vacuum for 3 days. It should be pointed out that the $CaCO_3$ synthesized in this way may have different characteristics from $CaCO_3$ obtained from EICP, however, since $CaCO_3$ obtained from EICP may contain other organic phases that could interfere with the protein adsorption study, $CaCO_3$ was synthesized and used in the adsorption experiment.

2.1.4. *EICP solution formulation*

EICP solution in this study was prepared by dissolving anhydrous $CaCl_2$, urea, urease, and proteins into DI water. The molar ratio of $CaCl_2$ to urea was maintained at 0.75:1, thus, 1.5 M of $CaCl_2$ and 2 M of urea. These concentrations were chosen based on prior trials to result in effective $CaCO_3$ precipitation in the test tube experiments carried out in this study. A high urease enzyme with an activity of 72,520 U/g was used in the EICP formulation. The urease enzyme solution was designed to achieve concentrations of 6 kU/L (1 U corresponds to the amount of enzyme that hydrolyses 1 µmol of urea per minute at pH 7.0 and 25 °C [85]) and 12 kU/L (Sigma Aldrich Type III Jack Bean Urease). These concentrations of urease were chosen to understand the effect of high and low urease concentrations on the mechanical and microstructural

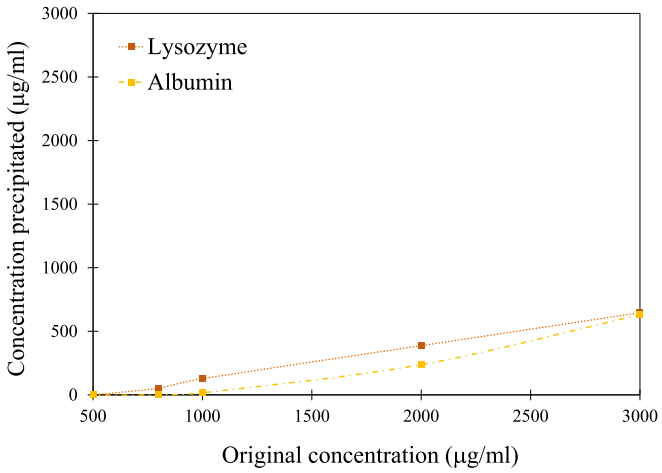

Fig. 8. Amount of proteins precipitated in the insoluble protein-Ca^{2+} complexes in the pore solution.

properties of the ground hardened cement paste.

The proteins used in the experiment were added at a concentration of 2% by mass of DI water. The stock solutions were prepared by first, mixing the appropriate mass of each protein with $CaCl_2$ and urea for 3 min in 25 mL DI water and then, mixing them with the already prepared 25 mL urease solution. Since the EICP process is fast, the stock solution was quickly poured into the mold containing the ground hardened cement paste.

2.1.5. Ground hardened cement paste treatment with EICP

Four replicates of the control and protein modified EICP-ground hardened cement paste were prepared using each of the stock solutions. Right after mixing the stock solutions, they were poured into the cylindrical molds and thoroughly mixed with the ground hardened cement paste. Fig. 2 illustrates the treatment cycle of the ground hardened cement paste. The ground hardened cement paste-EICP mixture was gently tamped so that the treated ground hardened cement paste column in the cylindrical mold reached a final height of 25 mm above the base. Following a slight compaction, the water level remained about 15 mm above the surface of the ground hardened cement paste column. The top of each column was covered with the parafilm foil to minimize solution loss by evaporation. In the case of the stock solution prepared with the 6 kU/L urease concentration, three treatment cycles were carried out. Treatment solutions were poured into the ground hardened cement paste column and drained after 12 hours. This was done on three occasions. On the third day after the treatment process, the solution was drained, and the column samples were oven-dried at 38 °C for 7 days. For the samples with the 12 kU/L urease concentration, only one cycle was applied. The column samples were kept at room temperature (23 °C) for three days; then solutions were drained out of the columns and the columns were oven-dried at 38 °C for 7 days. After 7 days, the samples were demolded and then prepared for further experimental investigation. Samples obtained from the interior of the columns were used to study the chemical characteristics and microstructure of the samples. A whitish powder was observed to form on the top surface of the columns; these precipitates were expected to result from the EICP solution remaining above the columns and thus contained less particles of ground hardened cement paste. Samples obtained from these precipitates on the top surface of the columns were also used in the FTIR and SEM tests.

2.2. Methods

2.2.1. pH measurement

The pH of the ground hardened cement paste treated with EICP solution with different proteins at different times was measured using a pH meter. The pH of the $CaCl_2$ and urea solution of concentrations 1.5 M and 2 M, respectively, was also measured. Prior to the pH measurement, the pH probe was calibrated with pH buffers of pH 4.0 and 7.0, respectively. After mixing the EICP solution with the ground hardened cement paste, the mixture was mixed and allowed to stand for one minute and then, the pH probe was dipped into the supernatant. After 24 and 48 hours, the pH probe was again dipped into the supernatant to measure the respective pH values. At these times, the reaction had completed.

2.2.2. Zeta potential and hydrodynamic size measurement of proteins

The net surface charge and the hydrodynamic size of the proteins were measured using a Zetasizer Nano ZS instrument (Malvern Instruments Ltd., Malvern, U.K.) at 25 ℃. In this experiment, the protein solutions with a 0.15% concentration by mass of DI water (native state) was prepared and their net charge and size determined. To simulate the pH of the cement environment and also to determine the effect of high pH on the proteins, the charge and size of the proteins were also determined at pH of 12.5. The solution was placed in a disposable folded capillary cell (DTS1070) that was loaded into the instrument. Each sample was tested 3 times with an equilibration time of 120 s inside the instrument before data was collected between 100 and 110 runs. The concentration of the proteins for the zeta potential analysis was the same as for the hydrodynamic size analysis. The measurement parameters for the zeta potential and hydrodynamic size analysis, namely, refractive index (RI) and absorption for the proteins was set at 1.45 and 0.001, respectively.

2.2.3. Surface adsorption and Ca^{2+} complexation measurement

The concentration of proteins adsorbed on the ground hardened cement paste, $CaCO_3$ and those that formed insoluble complexes with calcium ion were measured using the Agilent 8453 UV–Vis spectrophotometer at 25 ℃. The wavelength of 562 nm was used for the quantitative analysis since it is ideal for protein quantification analysis using the Bradford protein assay (BCA) [86,87]. The protein adsorption was measured using BCA [88,89]. The concentration of protein present is determined by measuring the absorption spectra of an unknown protein sample and comparing it with that of a known protein concentration [86]. The stability of the reagent under alkaline conditions makes the BCA method most suitable for the adsorption measurements [87]. For the protein adsorption tests on the ground hardened cement paste, 0.4 mL of DI water was mixed with 0.5 g of ground hardened cement paste, centrifuged, and left to stand for 20 min to allow the hydration of the unhydrated portion of the ground hardened cement paste. After 20 min, 0.1 mL of each of the protein solutions was mixed with the ground hardened cement paste mixture and centrifuged for one minute. The mixture was ultra-sonicated for 25 min. After ultra-sonication, the paste was centrifuged for 10 min. 0.1 mL of the supernatant was mixed with 2 mL of BCA reagent and incubated for 30 min at 37 ℃. After incubation, the mixture was cooled for 10 min at room temperature. A purple color indicated the presence of protein in the solution [87]. The concentration of protein adsorbed on the ground hardened cement paste was calculated from the difference between the concentration of protein in the equivalent volume of DI water only and the concentration of the supernatant. The adsorption experiment on the chemically synthesized $CaCO_3$ was conducted the same way as on the ground hardened cement paste except that instead of 0.4 mL of DI water, 0.4 mL of an extracted cement pore solution of the ground hardened cement paste was mixed with 0.5 g of $CaCO_3$. The extracted pore solution was filtrated from the mixture of ground hardened cement paste and DI water at a solid/water of (10g/30g). The final pH obtained was 12.66. The mixture was centrifuged to obtain the supernatant pore solution. Readings were taken in duplicates. It has previously been established that carboxylate groups may chelate Ca^{2+} in solution [90,91]. When the proteins are added to the ground hardened cement paste mixed with

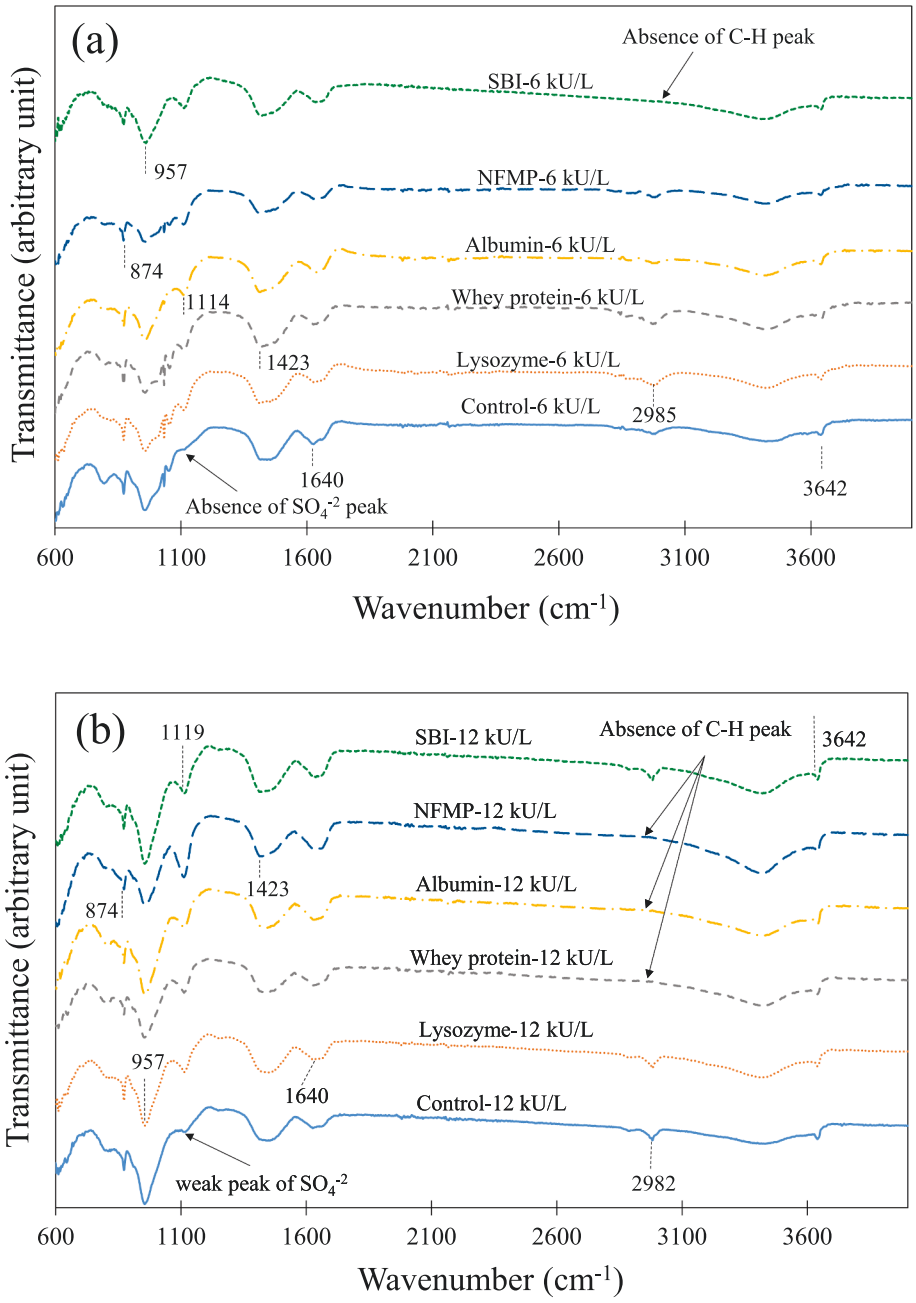

Fig. 9. FTIR spectra of the control and modified ground hardened cement paste treated with EICP with 2% protein using (a) 6 kU/L and (b) 12 kU/L urease concentrations.

water, complexes which are either water soluble or insoluble can be formed due to the reaction between carboxylates and Ca^{2+}. If insoluble products are formed, which are then precipitated from the solution phase, the adsorption measurement as described above can give wrong results because the complexes contained in the precipitates is falsely considered as the adsorbed protein on cement surface. Thus, the adsorbed concentration of the proteins on the ground hardened cement paste would be overestimated. To confirm whether complexes were formed, an extracted pore solution from the ground hardened cement paste (w/c of 1) was mixed with lysozyme, whey proteins, albumin, NFMP, and SBI, respectively. The amount of insoluble protein-Ca^{2+} complexation was determined from the difference in the concentration of proteins present in the original protein solution and after mixing with the extracted pore solution.

2.2.4. *Surface tension*

The surface tension test was carried out to study the surface hydrophobization of the proteins. Xiao et al. [92] established a direct correlation between surface tension and protein hydrophobicity. Solutions with 2% concentration of protein and 2 M concentration of urea were prepared and equilibrated for 5 min. The surface tension of the solutions was determined by the Wilhelmy Plate method [93,94] using an automated surface tension meter (BZY-102). Three tests were carried for each sample and the average reported.

2.2.5. *FTIR*

FTIR was used to study the chemical characteristics of the reaction products. The presence and intensity of the various polymorphs of $CaCO_3$ can be studied using the FTIR spectra. Samples obtained from the interior of the columns as well as from the precipitates on the top surface

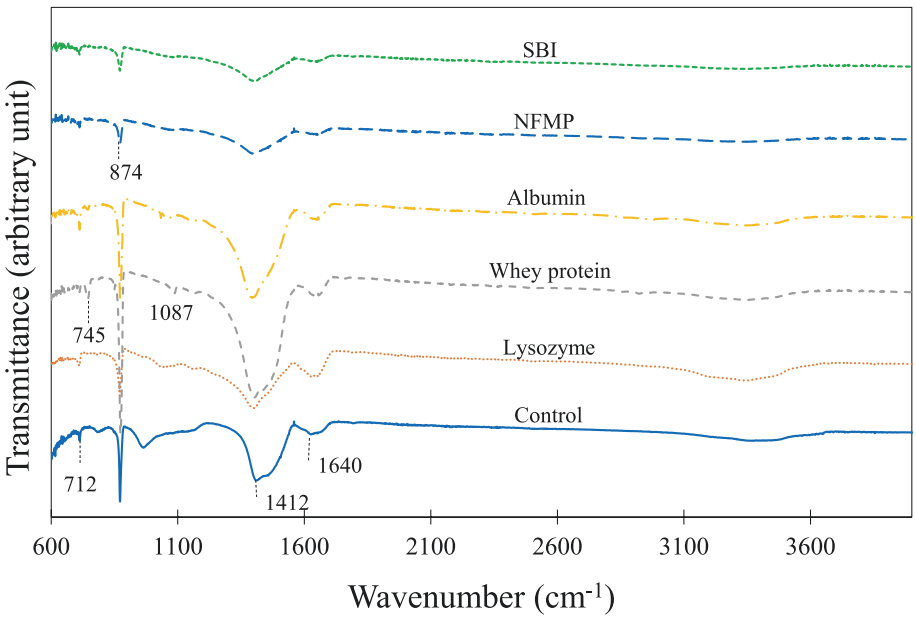

Fig. 10. FTIR spectra of the precipitates on the top of the control and modified ground hardened cement paste treated with EICP using 12 kU/L urease concentration with 2% protein.

of the columns were used (see Fig. 2b). Approximately 30 mg of the samples was ground and passed through the Sieve #60 and oven-dried at 50 °C in a vacuum oven for one day. The analysis was carried out using a Perkin Elmer Paragon 1000 FTIR equipped with an ATR accessory. The transmission infrared spectra of the samples were recorded in the region between 600 cm^{-1} and 4000 cm^{-1} at a resolution of 4 cm^{-1} with 4 scans per sample. An average of two samples from the round of 4 scans are reported in this study.

2.2.6. Thermogravimetric analysis

The content of CH and $CaCO_3$ in the reaction products was studied using the TA Instruments TGA55. For this test, the samples were prepared using small pieces obtained from the interior part of the treated ground hardened cement paste. The samples were ground into powder and passed through the Sieve #60. To avoid carbonation, the samples were oven-dried at 50 °C in a vacuum oven prior to testing. Samples were tested within two days. TGA was conducted on approximately 37 mg of each sample at a temperature increment of 20 ℃ per minute between 25 ℃ and 900 ℃ in an inert nitrogen atmosphere. Two replicates were used in this test.

2.2.7. Scanning electron microscopy

Small pieces obtained from the interior of the columns and precipitates obtained from the top of the columns were imaged in a SEM JEOL JSM-7000F. The precipitates were first passed through the Sieve #60 before imaging. The samples were placed on a carbon tape attached to a stub. The surfaces of the samples were coated with a thin layer of gold to reduce the effect of charging for high magnification imaging. The accelerating electron voltage was between 10 kV and 15 kV, and the working distance was 10 mm.

2.2.8. Micro-CT microscopy

Micro-CT microscopy was employed to provide more detailed information about the pore structure of the samples non-destructively. A 20 mm thick slice cut from a 40 mm diameter cylindrical sample was scanned using the v |tome|x s240 neo machine through a complete rotation of 360° and at a resolution of 10 μm. The primary objective of this analysis was to obtain the total porosity and pore size distribution of the samples under investigation.

2.2.9. Tensile strength test

The tensile strength of the control and protein modified ground hardened cement paste was determined using the indirect tensile test. Treated cylindrical specimens were removed from the molds and dried for 7 days before testing. Samples prepared with 6 kU/L and 12 kU/L urease concentrations and with or without proteins were used. The test was performed using an Intron machine at a loading rate of 0.005 mm/sec. The average of four replicates was calculated and reported in this study.

2.2.10. Water permeability test

The water permeability of the samples modified with EICP with 12 kU/L urease concentration and with or without proteins was investigated. Briefly, water pressure was generated on top of the specimens by means of a water column. Ingress of water through the sample was determined by recording the time as the water column seeps. The specimens already cast in a polyvinyl chloride (PVC) mold were sealed and mounted on a 100 mL measuring cylinder to collect the seeping water and to minimize evaporation. A 50 mL test tube was fixed on the surface of each specimen using a water sealant. The top of the specimen and the test tube were covered with a parafilm to minimize evaporation from the surface. The drop in water level in the test tube due to water flow through the samples was measured at the times of 10, 30, 60, 120, 180 and 240th minutes. These times were chosen based on pre-trials. The initial water head was measured to be 7.3 cm. For each samples, three replicates were used and the average reported.

3. Results and discussion

3.1. pH measurement

The pH of the ground hardened cement paste treated with EICP solutions at different times is shown in Fig. 3. The pH of the $CaCl_2$ urea solution was 10.31 at the initial stage but reduced after the solution was mixed with the various proteins indicating that the proteins are acidic in nature. The pH rose above 12 after mixing the $CaCl_2$-urea solution with the urease and ground hardened cement paste. The optimum pH of EICP solution is approximately 9.6 [95] which is relatively lower than the pH of EICP modified ground hardened cement paste. The increased pH is attributed to the release of hydroxyl ions (OH^-) due to the rehydration of

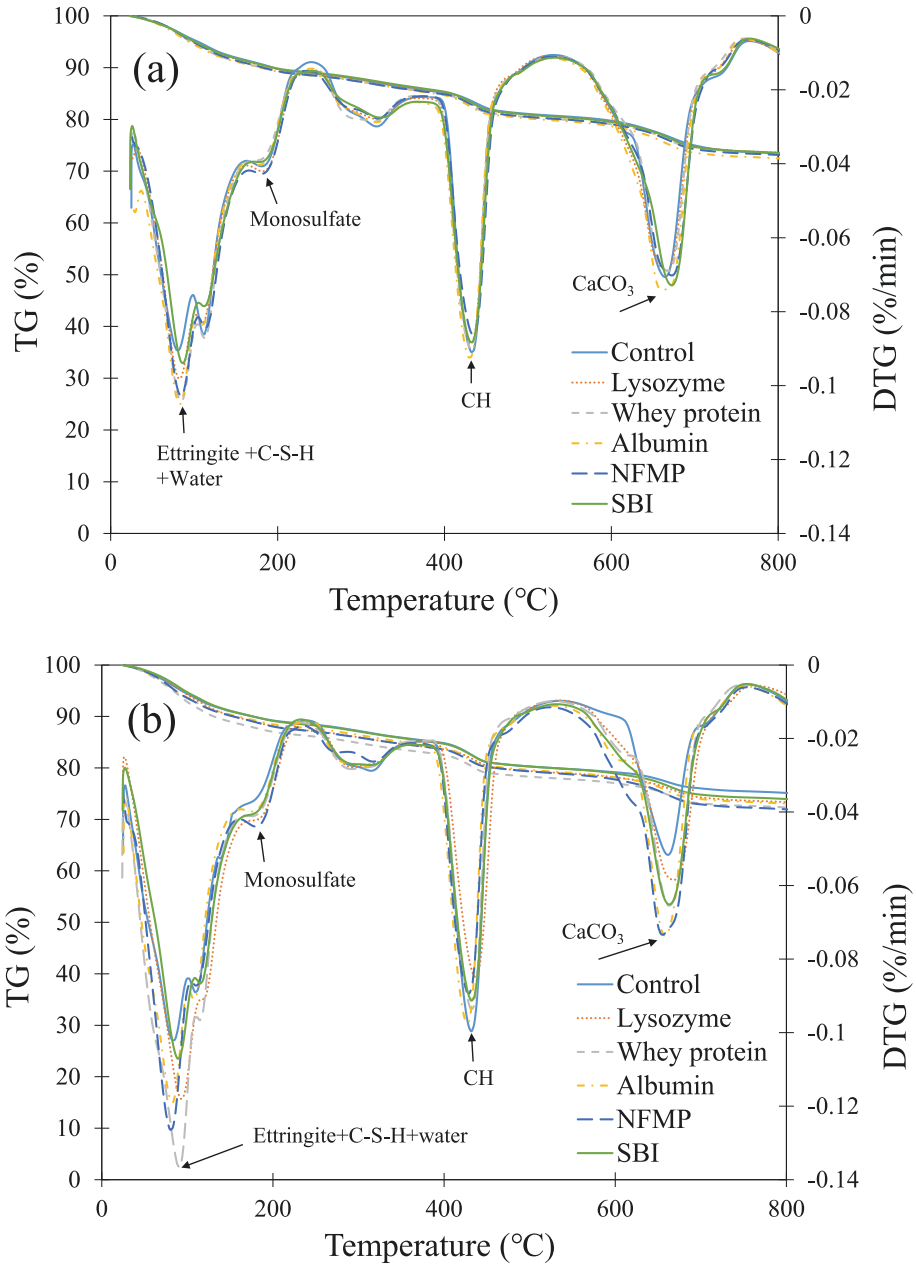

Fig. 11. TG and DTG curves of the control and modified ground hardened cement paste treated with EICP with 2% protein using (a) 6 kU/L and (b) 12 kU/L urease concentrations.

ground hardened cement paste [96].

The pH remained approximately at this level throughout the 72-hour period before draining them out for oven-drying. The measured pH of the solution extracted from the ground hardened cement paste and water was 13.06. Wan et al. [97] measured and reported that the pH of hardened concrete is slightly above 13 and it is independent of the age of the hardened cement paste. The slight reduction in pH of both the control and the protein modified samples after adding urease to the mixture is attributed to precipitation of the $CaCO_3$.

3.2. Zeta potential and hydrodynamic size

Net charge is a critical characteristic that affects the interactions between proteins and the solid particles. In view of this, the zeta potential of the proteins was investigated based on the electrophoretic mobility measurements [98]. The results obtained for the cationic and anionic charge of the proteins, measured at their native state and pH = 12.5 are shown in Fig. 4. It can be observed that the net anionic charge of the proteins increased with increasing pH; however, the change in charge was small in the case of SBI. The anionic charge increase is a function of the composition of the amino acid functional groups in the proteins. In their native states, whey protein, albumin, NFMP, and SBI, exhibited a net surface charge less than −25 mV while lysozyme showed a zeta potential value of + 22.6 mV. At pH of 12.5, whey protein, albumin, NFMP and SBI were characterized by zeta potential values of more than −30 mV, except lysozyme which showed zeta potential value of −15.6 mV. In general, absolute values of zeta potential more than 30 mV are required for colloidal particles to be considered stable against electrostatic aggregation [99]. The observed increase in zeta potential as a function of pH is attributed to the deprotonation of the amino acid functional groups in the proteins at pH of 12.5 [100,101]. The increase in negative charge at high pH was more pronounced in the case of lysozyme. Lysozyme showed a positive charge in its native state but became negatively charged as the pH increased to 12.5. Lysozyme has an

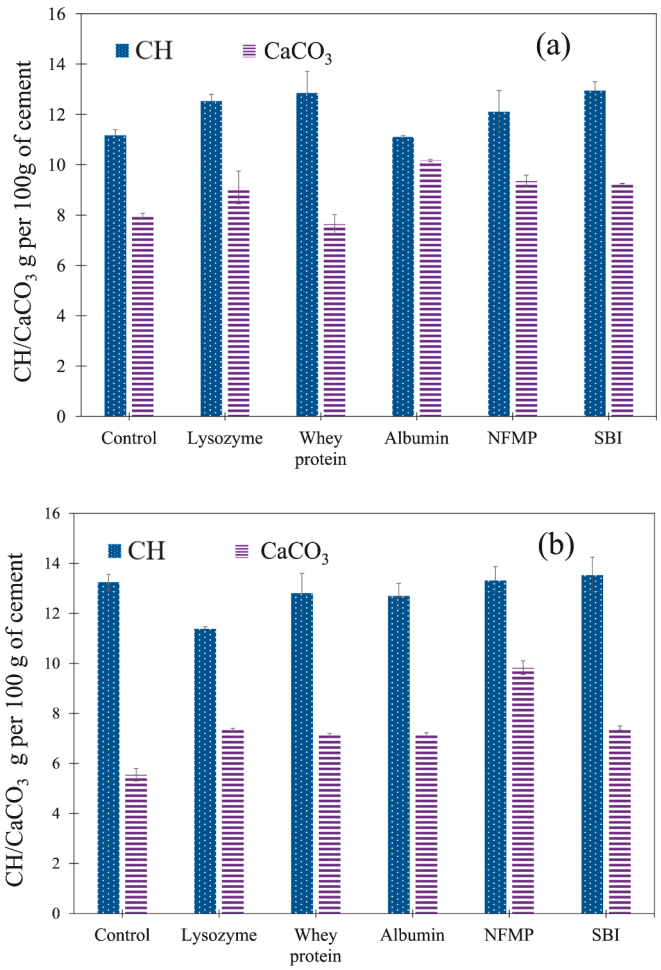

Fig. 12. CH and $CaCO_3$ quantification of the control and modified ground hardened cement paste treated with EICP with 2% protein using (a) 6 kU/L and (b) 12 kU/L urease concentrations.

isoelectric point of 11 [102]. Below this pH, lysozyme carries positively charged amino acid groups making the overall net charge of this protein positive [103].

The hydrodynamic size distribution by volume of the proteins in their native state and at pH = 12.5 is shown in Fig. 5. It is seen that lysozyme and whey showed an increase in particle size at pH = 12.5, compared to their native state. On the other hand, albumin, NFMP, and SBI exhibited an opposite behavior and their size decreased at pH = 12.5 compared to their native state; however, this size reduction was less pronounced in the case of SBI.

Increase in pH results in conformational changes in the molecular structure of proteins [104,105]. The reduction observed in the size of albumin, NFMP, and SBI may be attributed to the structural collapse and or dissociation of the protein aggregates that occur in the high pH environment. In addition, the increase in the negative zeta potential of these proteins at high pH is expected to increase repulsion between the protein thereby reducing aggregation, which leads to smaller sizes [106,107]. Li Wang et al. [108] studied the influence of pH on the hydrodynamic size of egg white/yolk. They observed a decrease in size as the pH level increased and attributed this phenomenon to the dissociation of the proteins at high pH. It must be emphasized that different proteins have different pH levels at which they begin to de-aggregate. For instance Soybean globulins is known to de-aggregate at pH 11.0 [109].

The observed increase in the size of lysozyme could be caused by a reduction in the absolute value of its surface charge at high pH compared to the native state. As mentioned above, a reduction in the surface charge decreases the repulsive forces between proteins, which increases protein tendency to aggregate. In the case of whey protein, the increase in size could be attributed to the re-association of the dissociated protein subunits to crossed linked network aggregate formation [101].

It should be noted that the proteins used in these studies were used as received, and they may have contained impurities to different extents; the impurities could favor the assembly of whey protein at high pH compared to its natural state. The change in size at high pH was small in the case of SBI; an explanation for this could be the small change observed in the charge of SBI at high pH compared to its natural state. Thus, the change in size due to change in electrostatic repulsive forces between SBI particles was not likely to occur.

3.3. Surface adsorption and Ca^{2+} complexation measurement

The adsorption measurements of the proteins including lysozyme, whey protein, albumin, NFMP and SBI on the ground hardened cement paste and $CaCO_3$ were obtained by UV–Vis spectrophotometry. As shown in Fig. 6, it is clearly observed that all the proteins except lysozyme showed maximum adsorption on the ground hardened cement paste. The adsorption characteristics of lysozyme could be due to its lower negative charge (see Fig. 4) compared to the other proteins. It has been reported that the adsorption of polymeric admixtures on cement grains is related to the charge types and the charge density in the molecules of the admixture [110]. In this study, the ground hardened cement paste used was 28 days old. The surface of these particles consisted of hydrated and unhydrated parts. For a 28 day age cement paste, it is generally expected that the main hydration products consist primarily of calcium-silicate-hydrate (C-S-H) and calcium hydroxide (CH) [111]. As a result of the continued hydration of the unhydrated part of the surface, Ca^{2+}, SO_4^{-2} and OH^- ions begin to diffuse into the solution between the particles first, and then silicates start to diffuse as well [112]. Eventually, the concentration of various ions in the solution increases. When the concentrations of ions reach the supersaturation criteria for the precipitation, rehydrated products including ettringite, C-S-H and CH are formed in the EICP treated medium.

In a high electrolyte solution like cement pore solution, Ca^{2+} adsorb on negatively charged silicate surfaces (C_3S, and C-S-H), resulting in a positive zeta potential in these phases [113]. Ettringite has a positive zeta potential in the absence of sulfate ion adsorption [113]. This diversity of processes builds up a panoply of different charges on the surface of the ground hardened cement paste particle. It is anticipated that the specific interaction between proteins and ground hardened cement paste would mainly be driven by the electrostatic interaction between the negatively charged proteins and positively charged phases on the surface of the ground hardened cement paste.

The adsorption of proteins on $CaCO_3$ in the pore solution is illustrated in Fig. 7. $CaCO_3$ in this case was formed by the chemical reaction between $CaCl_2$ and $NaCO_3$ at pH level of 12.5. The surface of $CaCO_3$ in a high alkaline medium is expected to exhibit a negative charge; in the presence of Ca^{2+} in the solution, Ca^{2+} can bind onto the surface of $CaCO_3$ [98,114], which can potentially facilitate the surface adsorption of negatively charged proteins through electrostatic interactions. It is interesting to note that the adsorption of proteins onto $CaCO_3$ is significantly less than that onto ground hardened cement paste. The higher adsorption of the proteins onto ground hardened cement paste compared to $CaCO_3$ could be due to the nature of the surface charge distribution as well as the possibility of other interaction pathways between the proteins and ground hardened cement paste. In addition, the porous nature of the ground hardened cement paste increases the specific surface area for the adsorption of the proteins compared to $CaCO_3$.

The formation of insoluble complexes between the proteins and Ca^{2+} was also investigated. To this end, the adsorption experiments were performed with the proteins in the pore solution only without the

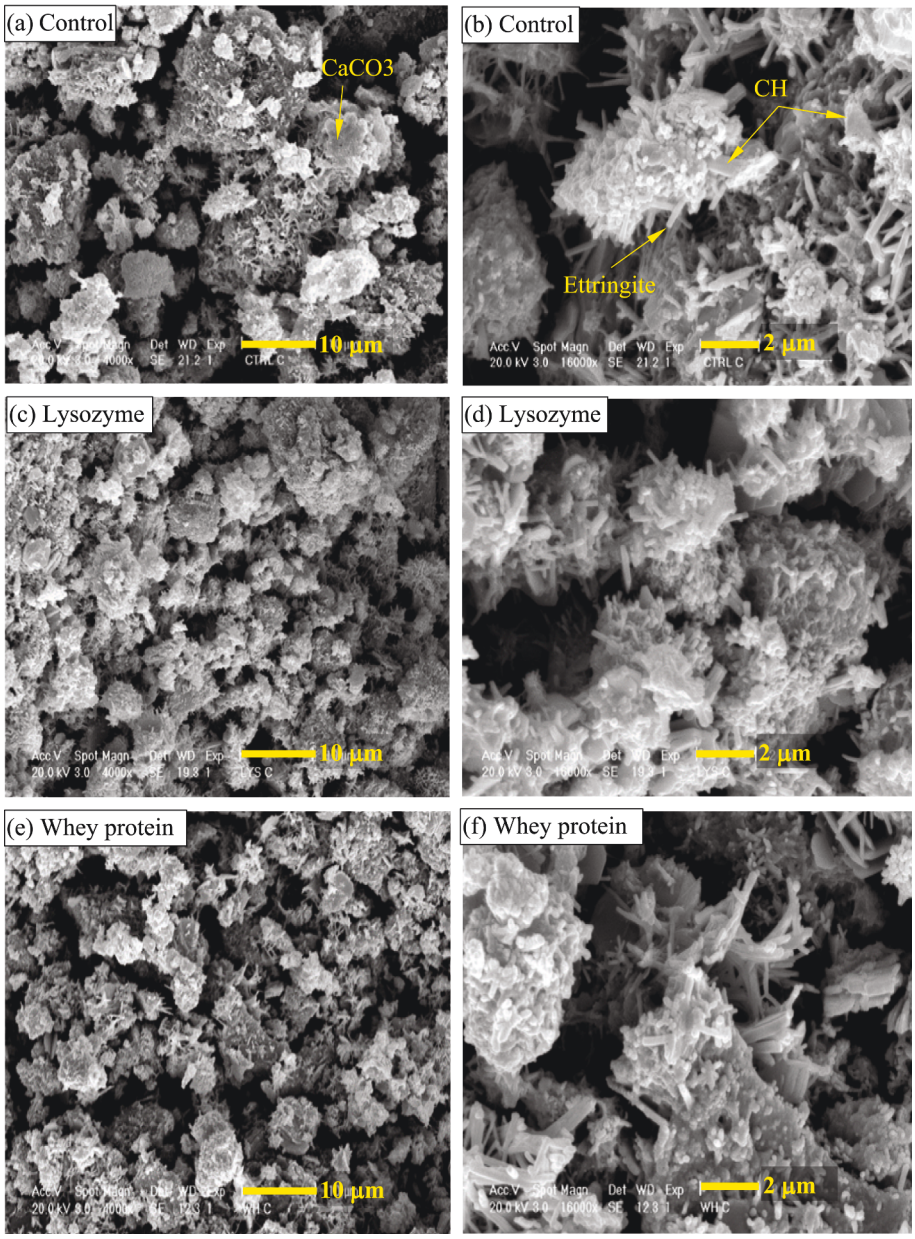

Fig. 13. SEM micrographs of the samples from the interior, taken at two magnifications of 4000X (a, c, e, g, i, and k) and 16000X (b, d, f, h, j, and l), of the control sample and the samples with proteins. These images correspond to the 12 kU/L urease concentration.

presence of any solid particles. Determination of the amount of insoluble protein-Ca^{2+} complexes in the solution allowed to distinguish these insoluble protein-Ca^{2+} complexes from proteins adsorbed onto the ground hardened cement paste or $CaCO_3$ surface. Because the difference in the concentration of dissolved proteins in the solution is used to determine the adsorption results, the insoluble protein-ion complexes could also contribute to the measured adsorption values, and this should be separately investigated. It is revealed from Fig. 8 that lysozyme and albumin formed some insoluble complexes with Ca^{2+} [115] present in the pore solution. It must be emphasized that whey protein and SBI showed very small values of concentration but were considered to be within the error margin of the experiment. It can be concluded that the proteins had a high affinity to ground hardened cement paste surface compared to $CaCO_3$ surface in the pore solution.

3.4. FTIR analysis

The chemical characteristics of the reaction products in the ground hardened cement paste treated with EICP was studied using FTIR. Fig. 9a and 9b illustrate the spectra of the ground hardened cement paste modified with 6 kU/L and 12 kU/L urease concentrations, respectively, and 2% protein, obtained from the core of the samples. In both FTIR analyses, the band at about 3642 cm^{-1} is caused by the stretching and bending bands of the hydroxyl (O − H) group that is attributed to the presence of CH in the EICP treated ground hardened cement paste [116,117]. In addition, the broad bands in the range of 3100 cm^{-1}-3600 cm^{-1} may correspond to the stretching of the O − H group contributed from water [116,117]. The characteristic peaks located at 2985 cm^{-1} and 2982 cm^{-1} are attributed to the stretching vibration of the carbon-hydrogen (C–H) group of the proteins and urea (organic compounds) which is located in the aliphatic hydrophobic side chain in the peptide

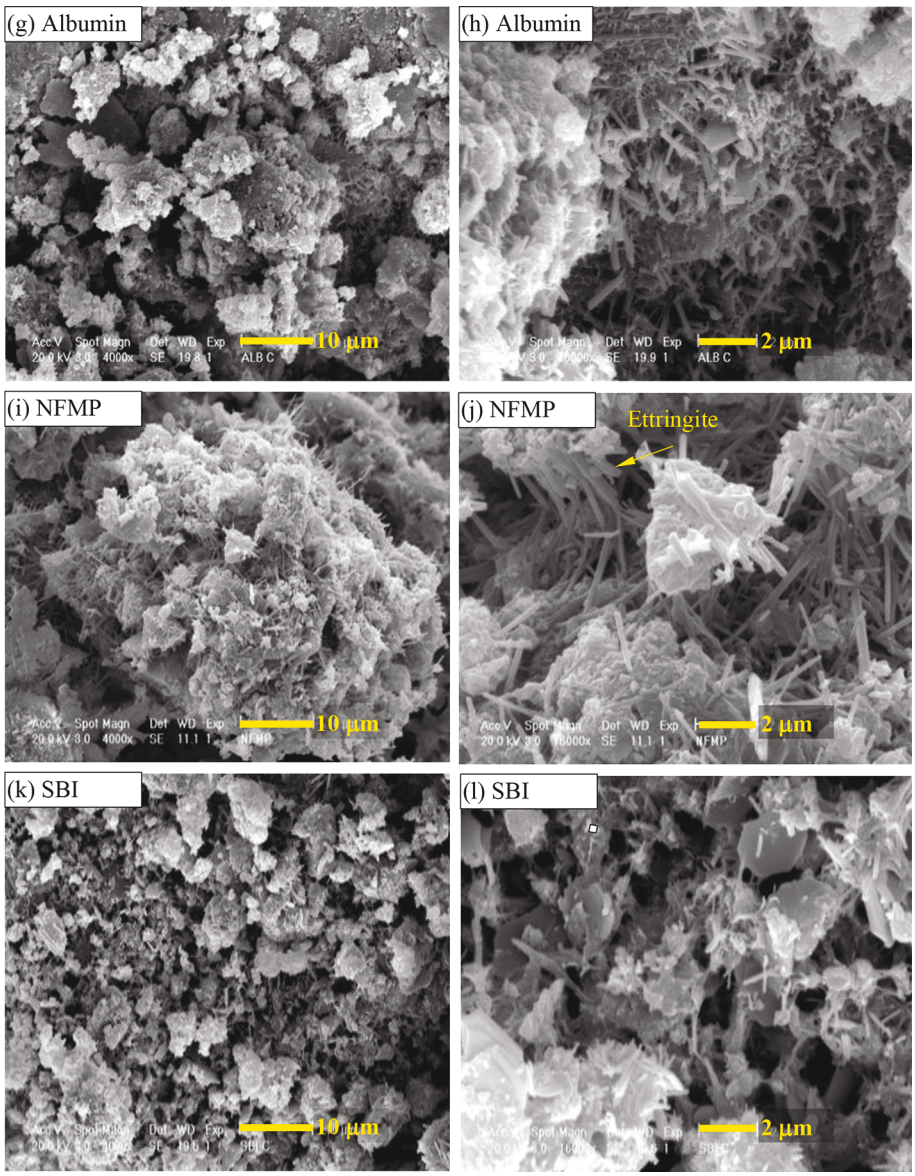

Fig. 13. (*continued*).

chain [118]. As shown in the spectra, there were disappearances or shift in this peak for some of the protein modified samples, indicating hydrophobic interaction between the proteins and the cement surfaces constituents [119,120]. The O – H of water and amide I both have peaks around 1640 cm^{-1} [116,120], however for O – H peak, the peak at 1640 cm^{-1} should be smaller than the peak at 3100 cm^{-1} –3600 cm^{-1}. Since O–H peak at 3100 cm^{-1} –3600 cm^{-1} is smaller than the peak at 1640 cm^{-1} in this instance, the peak is likely to be due to amide I due to the presence of protein and urea [120,121].

The characteristic peaks ranging between 1114 cm^{-1} and 1119 cm^{-1} of the control and protein modified ground hardened cement paste can be attributed to S-O stretching vibration (ν_3) of sulfate (SO_4^{-2}) in ettringite [117,122]. This peak is less pronounced in the control sample, compared to the samples modified with proteins. From Fig. 9b, it seems that the peak corresponding to ettringite in the spectrum of the sample modified with NFMP is larger than that in the spectra of other samples indicating a larger content of ettringite in the sample modified with NFMP than other samples. The out-of-plane bending located at 874 cm^{-1} and (ν_3) peak located at 1423 cm^{-1} in the control and the protein modified samples are attributed to the carbonate (CO_3^{-2}) bands [116,122]. A change in the shape of the (ν_3) peaks among the samples can be observed, which can be attributed to the effect of the proteins. Many researchers have reported a number of organic molecules that regulate nucleation, polymorphism and crystal growth of $CaCO_3$ in biological minerals [123,124]. The stretching vibration of Si-O-Si which is assigned to the peak at 957 cm^{-1} [125] is attributed to C-S-H in the samples.

The FTIR spectra of the samples obtained from precipitates on the top of the samples are shown in Fig. 10. As indicated previously, these deposits are expected to have a larger amount of $CaCO_3$ compared to the samples obtained from the core of the samples, which are mixed with ground hardened cement paste. This allowed us to obtain stronger peaks related to $CaCO_3$, which could assist in identifying possible polymorphs of $CaCO_3$ in the samples. The control sample showed a characteristic peak of calcite at 712 cm^{-1} and 874 cm^{-1} and a broad peak at 1412 cm^{-1}. Lysozyme, albumin and NFMP modified EICP exhibited characteristic peaks at 712 cm^{-1}, 874 cm^{-1} and 1412 cm^{-1} indicating the presence of calcite. The calcites identified as the only polymorphs in NFMP sample is in line with results reported by [72]. Interestingly, in addition to the calcite characteristic peaks of the whey protein modified samples, there were additional peaks at 745 cm^{-1} and 1087 cm^{-1}. These peaks correspond to the formation of vaterite [79].

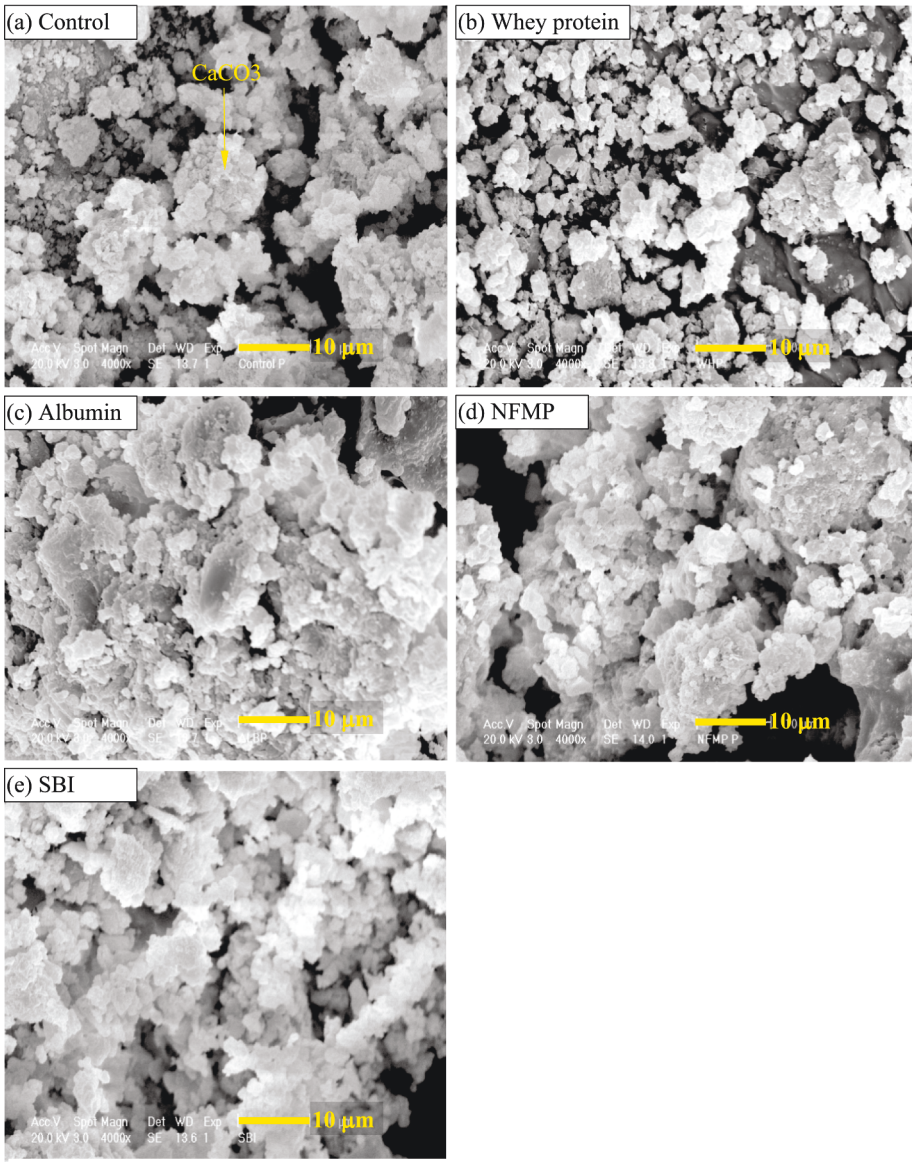

Fig. 14. SEM micrographs (a, b, c, d, e) of the precipitate obtained from the top of the samples corresponding to the 12 kU/L urease concentration with 2% protein concentration.

3.5. Thermogravimetric analysis

TGA was employed to further identify and quantify the phases present in the samples. Fig. 11a and 11b illustrate the TG and DTG curves of EICP treated ground hardened cement paste samples with and without 2% of protein treated with 6 kU/L and 12 kU/L of urease concentrations. Mass loss in the temperature below 100 °C is typically due to water evaporation. In the TG measurement, the main weight loss of ettringite (AFt) is around 100 °C while monosulfate (AFm) phase can be identified between 180 °C and 200 °C [126]. Chemically bound water loss of C-S-H occurred around 110 °C and 200 °C [127]. When the temperature increased from 410 °C to 480 °C, there was a noticeable mass loss in the TG profile. This can be attributed to the decomposition of CH [128,129]. The next mass loss is seen in the temperature range of about 620 °C to 720 °C, which is attributed to the decomposition of $CaCO_3$ [128,130]. Combined with the FTIR results, it seems that the main mineralogical phases present in the samples are ettringite, C-S-H, CH and $CaCO_3$. The quantification of CH and $CaCO_3$ contents in the control and protein modified samples is shown in Fig. 12a and 12b. It is observed that the protein modified samples generally showed a higher $CaCO_3$ content compared to the control samples in both the 6 kU/L and 12 kU/L urease concentrations. Proteins can affect the precipitation of $CaCO_3$ in different manners. The adsorption of proteins to solid phases including ground hardened cement paste provides nucleation sites for $CaCO_3$ resulting in increased $CaCO_3$ precipitation in the mixture. In addition, the binding of Ca^{2+} to the negatively charged segments of proteins in the solution leads to a local increase of Ca^{2+} concentration, and as a result, higher supersaturation, in the negative charged segments, compared to the bulk of the solution, thus promoting precipitation of $CaCO_3$ [131]. However, it should be noted that in a recent study by Almajed et al. [72], use of NFMP was shown to decrease the $CaCO_3$ content of EICP applied to Ottawa soil, which is comprised of 99% silica sand. There were major differences between our case and the above-mentioned study; first, pH of the mixture in our case was about 12.5, which was higher than that used in the above-mentioned study (less than 10); second, the surface characteristics of ground hardened cement paste are different from non-reactive silica sand. These could explain the reason for the opposite trend observed in the effect of NFMP on EICP in our case, compared to the above-mentioned study. There are mechanisms by which proteins can inhibit precipitation or growth of $CaCO_3$. Gelation of Ca^{2+} with

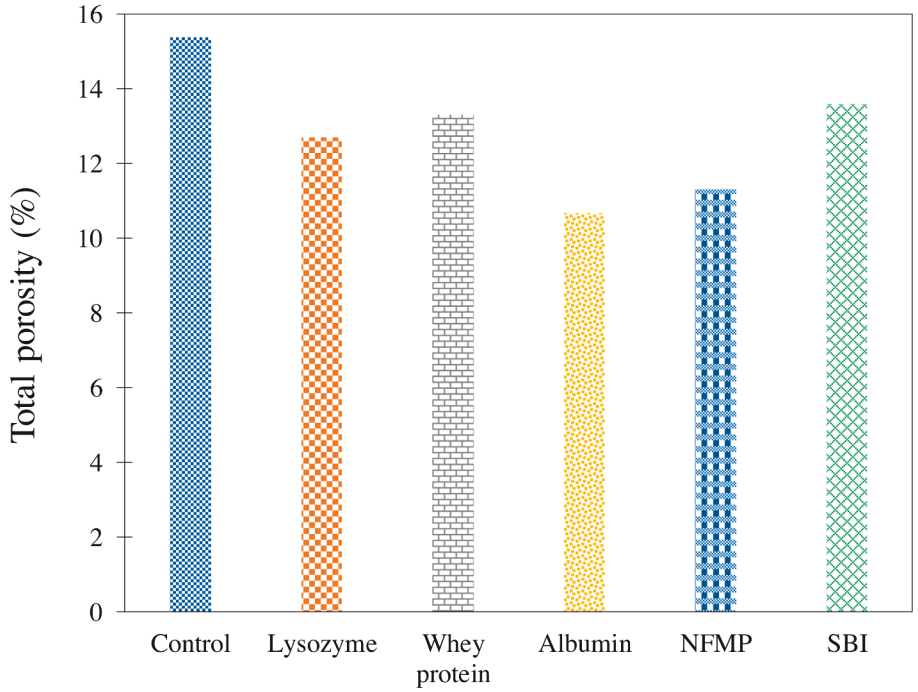

Fig. 15. Total porosity of the control and 2% protein concentration modified samples prepared with 12 kU/L of urease concentration.

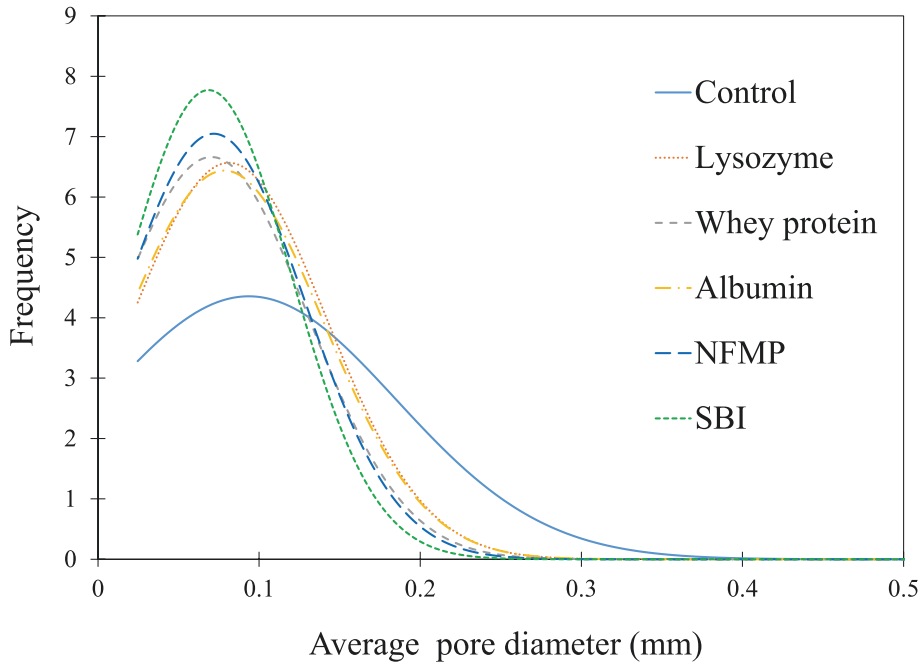

Fig. 16. Pore size distribution of the control and 2% protein concentration modified samples prepared with 12 kU/L urease concentration.

negatively charged protein could reduce the available Ca^{2+} in the bulk solution leading to a reduction in $CaCO_3$ precipitation. The selective adsorption of proteins onto $CaCO_3$ surfaces can inhibit crystal growth [131]. Nonetheless, as shown in Fig. 12a and 12b, the overall effect of protein favored an increase in the precipitation of $CaCO_3$ over the duration of the experiments. Since the samples with 6 kU/L urease concentration underwent 3 cycles of EICP treatment, they generally showed a slightly higher $CaCO_3$ content, compared to the samples with 12 kU/L urease concentration, which underwent only one cycle of EICP treatment.

3.6. Scanning electron microscopy

SEM microscopy was utilized to investigate the microstructural features of the samples. SEM images, taken at two magnifications of 4000X and 16000X, of the control and protein modified ground hardened cement paste with 12 kU/L urease concentration are shown in Fig. 13a-13 l. It is generally observed from the images that rod-like features are present in the microstructure. These features are likely to be ettringite [111]. There is also the appearance of hexagonal shaped features, which resemble crystals of CH [111]. Also shown in the SEM images, are $CaCO_3$ produced due to EICP and potentially carbonation of CH as a result of

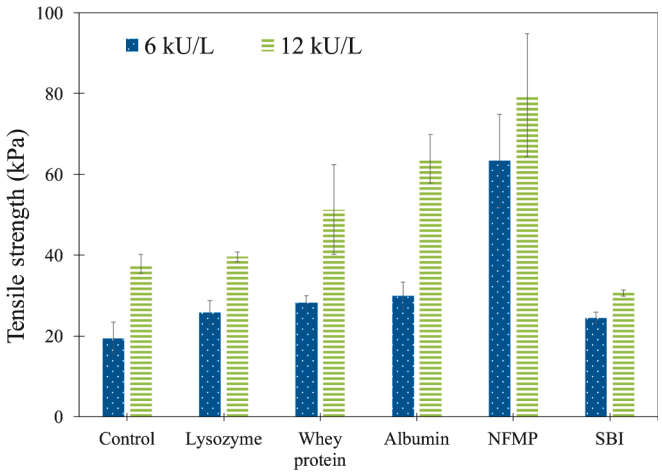

Fig. 17. Tensile strength of the control and protein modified samples at 6 kU/L and 12 kU/L urease concentrations with a protein concentration of 2%.

continued hydration of unhydrated ground cement paste. From the examination of the SEM images taken at the 4000X magnification, it is seen that the microstructure of the control sample appears to be less densified compared to that of the samples modified with proteins. This is evident from larger interspacing between features seen in the microstructure of the control sample, compared to those in the samples modified with proteins. The SEM images of the samples modified with NFMP are shown in Fig. 13i and 13j. From these images, a more pronounced presence of ettringite is observed in the sample modified with NFMP than in the other samples. This observation seems to be in agreement with the FTIR results discussed previously.

SEM micrographs of precipitates obtained from the top of the samples prepared with 12 kU/L of urease concentration with or without 2% protein concentration are shown in Fig. 14 a-e; as indicated previously, since these precipitates were formed in the pore solution deposited at the top of the samples that had smaller number of solid ground hardened cement paste particles, it was comprised of a larger content of $CaCO_3$, which allowed for better examination of their morphology in the SEM examination without being obscured when mixed with ground hardened cement paste particles. SEM images shown in Fig. 14 a-e confirmed the formation of $CaCO_3$, and that calcite was the main polymorph formed in the control sample and the samples modified with proteins. Formation of calcite as the primary polymorph is consistent with prior studies, which suggested that when EICP is precipitated on solid particles, calcite crystallization is favored [132]. In a bulk solution, inclusion of proteins favors formation of vaterite; however, when solid particles are present in the solution as observed in the ground hardened cement paste, calcite formation is favored [132,133]. This indicates that in addition to the chemistry of the pore solution, the presence and surface characteristics of the solid particles in the medium play an important role in $CaCO_3$ phases. Although whey protein modified samples showed some peaks

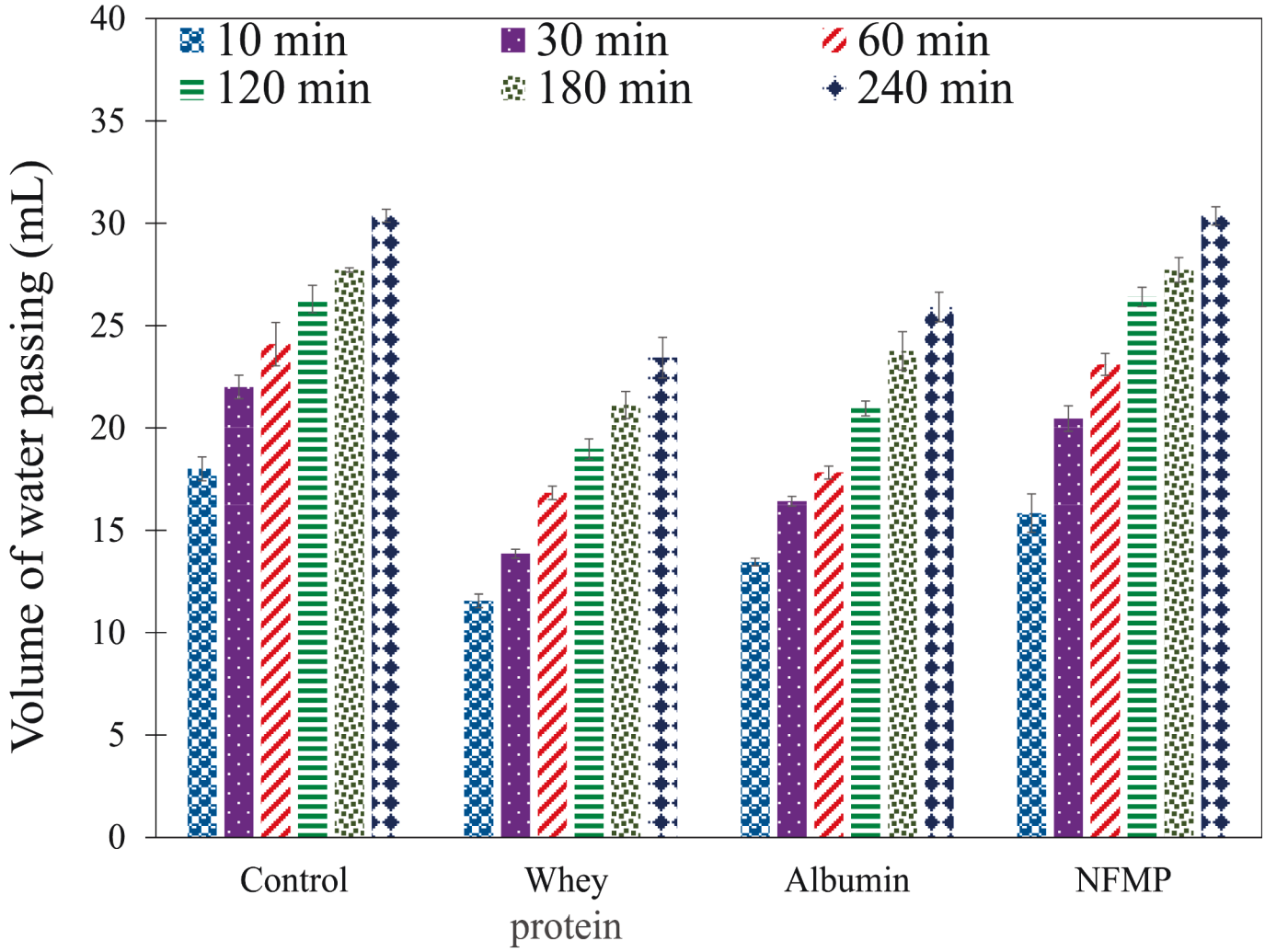

Fig. 18. Volume of water passing through the control and protein modified samples with 12 kU/L urease concentration prepared with protein concentration of 2%.

corresponding to vaterite in the FTIR analysis (Fig. 10), vaterite could not be identified in the SEM micrographs.

3.7. Micro-CT analysis

Figs. 15 and 16 illustrate the total porosity and pore size distribution of the 12 kU/L of urease concentration samples determined by the micro-CT analysis. Treated samples were modified with 2% protein concentration. The total porosity of the control, lysozyme, whey protein, albumin, NFMP and SBI modified samples was 15.37%, 12.7%, 13.3%, 10.67% 11.3% and 13.6%, respectively. It can be observed that the total porosity of the samples modified with proteins was lower than that of the control sample, with the albumin and NFMP modified samples exhibiting the lowest porosity. The average pore diameter of the control sample as shown in Fig. 16 was 0.094 mm, whereas the average pore diameter of the protein modified samples was 0.081 mm, 0.070 mm, 0.078 mm, 0.072 mm, and 0.068 mm for lysozyme, whey protein, albumin, NFMP and SBI, respectively. The less densified microstructure of the control sample as reported in the SEM, is consistent with the higher porosity and pore size of the control sample.

The decrease in the total porosity of the samples modified with proteins could be in part due to an increase in $CaCO_3$ in the samples modified with proteins, compared to the control sample, as evidenced from the TGA results. The more pronounced reduction in the pore size distribution in the samples modified with proteins can be attributed to the more uniform precipitation of $CaCO_3$ in the microstructure. The adsorption of proteins on the surface of ground hardened cement particles provides nucleation sites for $CaCO_3$, which leads to a more uniform $CaCO_3$ precipitation and smaller interspace between the precipitates. The adhesive and cohesive behaviors of the proteins, which can serve as a glue between solid phases in the microstructure can also contribute to the observed smaller pore distribution. The adsorption of the proteins onto $CaCO_3$ could affect the precipitation kinetics resulting in a more stabilized precipitation of $CaCO_3$ from the solution, and as a result more uniform distribution of the precipitates in the microstructure.

3.8. Tensile strength

The tensile strength of the control sample and the samples modified with 2% proteins is shown in Fig. 17. This Figure shows the result corresponding to the 6 kU/L and 12 kU/L urease concentration samples, respectively. Ground hardened cement paste sample prepared without EICP showed no strength and as such, is not plotted. This indicated that the reaction products resulting from continued hydration of ground hardened cement paste was not able to provide adhesion between the particles. The observed increased tensile strength of the samples treated with EICP can be attributed to the EICP, which precipitated and bonded the loosely ground hardened cement paste particles.

It can be observed from Fig. 17 that generally, the samples modified with proteins showed a higher tensile strength than the control samples. The increase in tensile strength was more pronounced in the samples modified with NFMP, followed by albumin, whey protein and lysozyme, respectively. This increase was more evident in the case of 12 kU/L than 6kU/L urease concentrations, as seen from Fig. 17. The higher strength of the samples with NFMP is in agreement with the results discussed in recent studies where EICP modified with NFMP was applied to silica sand [72,133].

The reduced porosity and average pore size of the samples modified with proteins compared to the control sample, as evidenced in Figs. 15 and 16 could be a contributing factor to the increased strength of these samples. It is interesting to note that the tensile strength of the albumin and NFMP modified samples follow the same trend as their respective reduced total porosities.

The adhesive strength of the proteins can play an important role in the binding of the constituents in the microstructure, and as such, the mechanical tensile strength of the samples. The importance of the adhesive strength brought about by the proteins can be realized from the higher tensile strength of the samples modified with albumin and NFMP, compared to the samples modified with other proteins even though the pore size distribution appeared to be similar for all sample with proteins. The reduced tensile strength of the samples modified with SBI can be attributed to a possible hydrolysis of SBI due to the combined denaturation effect of urea and high pH. Both urea and high pH are known denaturation agents [134]. The combined effect of these denaturation agents may reduce the adhesive strength of SBI. The adhesive properties of proteins in applications including wood have been studied in the past [135-137]. The adsorption of proteins or amino acids on $CaCO_3$ can lead to the formation of organic–inorganic bio-composites. Such composites have been reported by Cantaert et al. [138] and Mayer [139] to possess improved mechanical properties arising from their microstructural morphology directed by the biomolecules. It is plausible that in our case, some of the proteins resulted in protein-$CaCO_3$ composites that were able to provide enhanced interfacial strength between the ground hardened cement paste particles, and thus, improved the overall tensile strength of the samples. Several researchers including Ihsani et al. [74] and Almajed et al. [72] demonstrated an improvement in cracked concrete strength and soil strength, respectively, when NFMP was included in the EICP treatment solution. It should be noted that one clear observation which stood out for the sample modified with NFMP was the presence of more ettringite in the microstructure, as evidenced from SEM imaging and FTIR results discussed earlier. These rod-like features can act as fiber mineral fillers that can bridge between the structures, seal pores and enhance the strength of the samples. This could further enhance the tensile strength of the samples modified with NFMP.

3.8.1. Water permeability

Fig. 18 shows the volume of water passing through the samples with 12 kU/L urease concentration at 10, 30, 120, 180 and 240th minutes. Modified samples were prepared with 2% protein concentration. Lysozyme and SBI modified samples could not be used in the permeability test because the samples disintegrated and lacked cohesion at the start of the experiment due to the presence of water. This result appears to be in agreement with the lower tensile strength exhibited by the lysozyme and SBI modified samples as shown in Fig. 17. It is generally observed that the samples modified with whey protein and albumin showed lower reduction in water permeability compared to the control sample. The sample modified with NFMP showed lower water permeability at early times, but the difference diminished at late times. This could be attributed to the negative impact of moisture on the NFMP modified sample. Reduction in protein adhesion due to increased moisture content has been observed in prior study [135]. A systematic investigation on the adhesion properties of the proteins used in this study is under way and will be reported in the future publications.

A study by Nemati et al. [75] using EICP modified with skim powder, which is expected to be similar to NFMP, showed a reduction in the permeability of an unconsolidated porous media. However, in our case, the sample modified with NFMP was less effective in improving permeability, compared to the samples modified with other proteins.

The reduced water permeability in the samples modified with whey protein and albumin could be related to the microstructure; the micro-CT analysis, as discussed previously, indicated a smaller pore size distribution and total porosity in the sample modified with whey protein and albumin compared to the control sample. This difference in the microstructure can be a reason for the lower water permeability of the sample modified with whey protein and albumin compared to that of the control sample.

In addition, the hydrophobic property of proteins or polymers is capable of inducing water repelling effect on surfaces [140-143]. Xiao et al. [92] established a direct correlation between surface tension and protein hydrophobicity. It was reported that, as the surface tension of the protein solution decreased, the hydrophobicity of the protein increased due to the gradual exposure of the hydrophobic regions. From

the test results, the surface tension of urea only, whey protein, albumin and NFMP was 71.7 mN/m, 41.3 mN/m, 46.3 mN/m, and 49.7 mN/m, respectively. Among the proteins, NFMP showed the highest surface tension making it least hydrophobic followed by albumin and then whey protein. It is interesting to note that the effect of proteins on reducing the sample permeability followed the proteins' trend of reduced surface tension or increased hydrophobicity.

4. Conclusions

In this study the effect of proteins on EICP in binding ground hardened cement paste particles was studied. The major findings of the study are stated below.

- The zeta potential analysis showed an increase in negative charge when pH was increased to 12.5. The effect of increased pH on protein size was different for the proteins.
- Adsorption experiment revealed that high negative charge densities favored adsorption of proteins onto ground hardened cement paste. Proteins showed significantly smaller adsorption to $CaCO_3$, compared to the ground hardened cement paste.
- FTIR, TGA, and SEM analyses showed that ettringite, $CaCO_3$, and CH were the reaction products found in the sample. Calcite was identified as the main polymorph of $CaCO_3$ in the samples, and this was due to the high pH of the environment favoring the formation of calcite. It was observed that the samples modified with proteins exhibited a higher $CaCO_3$ content than the control sample. The sample modified with NFMP revealed a higher ettringite content compared to the sample modified with other proteins.
- The total porosity and average pore size were reduced for the samples modified with proteins compared to the control sample. This could be attributed to higher $CaCO_3$ content in the samples modified with proteins.
- Overall, the tensile strength of the samples modified with proteins was higher than that of the control sample. Tensile strength improvement was more pronounced in the samples modified NFMP, whey protein and albumin. Lower porosity and pore size distribution, and more importantly, improvements in the interfacial adhesion of the constituents provided by proteins could be the reason for enhanced tensile strength of the samples modified with proteins compared to the control sample.
- It was found that the sample modified with whey protein and albumin had a lower water permeability compared to the control sample. This could be explained in light of lower total porosity and smaller pore size distribution of the samples modified with these two proteins compared to the control sample. In addition, internal pore surface hydrophobicity induced by the proteins contributed to the lower water permeability of the samples modified with whey protein and albumin. Surface tension measurements of the protein solutions, as an indicator of their pore surface hydrophobization ability, seemed to show a good agreement with the effect of the proteins on reducing water permeability.

CRediT authorship contribution statement

Elvis Baffoe: Methodology, Data curation, Writing – original draft, Validation. **Ali Ghahremaninezhad:** Conceptualization, Methodology, Supervision, Writing – review & editing.

Declaration of Competing Interest

The authors declare that they have no known competing financial interests or personal relationships that could have appeared to influence the work reported in this paper.

Data availability

Data will be made available on request.

Acknowledgement

This study was supported in part by the National Science Foundation under the CAREER award number 1846984.

References

[1] K. Van Tittelboom, N. De Belie, W. De Muynck, W. Verstraete, Use of bacteria to repair cracks in concrete, Cem. Concr. Res. 40 (2010) 157–166.
[2] M. Biswas, S. Majumdar, T. Chowdhury, B. Chattopadhyay, S. Mandal, U. Halder, S. Yamasaki, Bioremediase a unique protein from a novel bacterium BKH1, ushering a new hope in concrete technology, Enzyme Microb. Technol. 46 (2010) 581–587.
[3] N. De Belie, E. Gruyaert, A. Al-Tabbaa, P. Antonaci, C. Baera, D. Bajare, et al., A review of self-healing concrete for damage management of structures, Adv. Mater. Interfaces. 1800074 (2018) 1–28.
[4] W. Tang, O. Kardani, H. Cui, Robust evaluation of self-healing efficiency in cementitious materials - A review, Constr. Build. Mater. 81 (2015) 233–247.
[5] T. Nishiwaki, M. Koda, M. Yamada, H. Mihashi, T. Kikuta, Experimental study on self-healing capability of FRCC using different types of synthetic fibers, J. Adv. Concr. Technol. 10 (2012) 195–206.
[6] B. Isaacs, R. Lark, T. Jefferson, R. Davies, S. Dunn, Crack healing of cementitious materials using shrinkable polymer tendons, Struct. Concr. 14 (2013) 138–147.
[7] A. Jefferson, C. Joseph, R. Lark, B. Isaacs, S. Dunn, B. Weager, A new system for crack closure of cementitious materials using shrinkable polymers, Cem. Concr. Res. 40 (2010) 795–801.
[8] M. Wu, B. Johannesson, M. Geiker, A review: Self-healing in cementitious materials and engineered cementitious composite as a self-healing material, Constr. Build. Mater. 28 (2012) 571–583.
[9] H.X.D. Lee, H.S. Wong, N.R. Buenfeld, Potential of superabsorbent polymer for self-sealing cracks in concrete, Adv. Appl. Ceram. 109 (2010) 296–302.
[10] D. Snoeck, S. Steuperaert, K. Van Tittelboom, P. Dubruel, N. De Belie, Visualization of water penetration in cementitious materials with superabsorbent polymers by means of neutron radiography, Cem. Concr. Res. 42 (2012) 1113–1121.
[11] G. Lefever, D. Van Hemelrijck, D. G. Aggelis, D. Snoeck, Evaluation of self-healing in cementitious materials with superabsorbent polymers through ultrasonic mapping, Constr. Build. Mater. 344 (2022) 1–11.
[12] P. Termkhajornkit, T. Nawa, Y. Yamashiro, T. Saito, Self-healing ability of fly ash-cement systems, Cem. Concr. Compos. 31 (2009) 195–203.
[13] S.H. Na, Y. Hama, M. Taniguchi, O. Katsura, T. Sagawa, M. Zakaria, Experimental Investigation on reaction rate and self-healing ability in fly ash blended cement mixtures, J. Adv. Concr. Technol. 10 (2012) 240–253.
[14] P. Anbu, C.-H. Kang, Y.-J. Shin, J.-S. So, Formations of calcium carbonate minerals by bacteria and its multiple applications, Springerplus. 5 (2016) 250.
[15] K. Van Tittelboom, N. De Belie, Self-healing in cementitious materials—a review, Materials (Basel). 6 (2013) 2182–2217.
[16] K. Sisomphon, O. Copuroglu, E.A.B. Koenders, Effect of exposure conditions on self healing behavior of strain hardening cementitious composites incorporating various cementitious materials, Constr. Build. Mater. 42 (2013) 217–224.
[17] T.-H. Ahn, T. Kishi, Crack self-healing behavior of cementitious composites incorporating various mineral admixtures, J. Adv. Concr. Technol. 8 (2010) 171–186.
[18] V.C. Li, E. Herbert, Robust self-healing concrete for sustainable infrastructure, J. Adv. Concr. Technol. 10 (2012) 207–218.
[19] C. Joseph, A.D. Jefferson, B. Isaacs, R.J. Lark, D.R. Gardner, Experimental investigation of adhesive-based self-healing of cementitious materials, Mag. Concr. Res. 62 (2010) 831–843.
[20] C. Dry, Matrix cracking, repair and filling using active and passive modes for smart times releases of internal chemicals, Smart Mater Struct. 3 (1994) 118–123.
[21] C.M. Dry, Three designs for the internal release of sealants, adhesives, and waterproofing chemicals into concrete to reduce permeability, Cem. Concr. Res. 30 (2000) 1969–1977.
[22] T. Nishiwaki, H. Mihashi, B.-K. Jang, K. Miura, Development of self-healing system for concrete with selective heating around crack, J. Adv. Concr. Technol. 4 (2006) 267–275.
[23] Z. Yang, J. Hollar, X. He, X. Shi, Laboratory assessment of a self-healing cementitious composite, Transp. Res. Rec. J Transp. Res. Board. 2142 (2010) 9–17.
[24] K. Van Tittelboom, N. De Belie, D. Van Loo, P. Jacobs, Self-healing efficiency of cementitious materials containing tubular capsules filled with healing agent, Cem. Concr. Compos. 33 (2011) 497–505.
[25] V. Wiktor, H.M. Jonkers, Quantification of crack-healing in novel bacteria-based self-healing concrete, Cem. Concr. Compos. 33 (2011) 763–770.
[26] C. Edvardsen, Water permeability and autogenous healing of cracks in concrete, ACI Mater. J. 96 (1999) 448–454.
[27] J.Y. Wang, N. De Belie, W. Verstraete, Diatomaceous earth as a protective vehicle for bacteria applied for self-healing concrete, J. Ind. Microbiol. Biotechnol. 39 (2012) 567–577.

[28] J. Wang, K. Van Tittelboom, N. De Belie, W. Verstraete, Use of silica gel or polyurethane immobilized bacteria for self-healing concrete, Constr. Build. Mater. 26 (2012) 532–540.
[29] J.Y. Wang, D. Snoeck, S. Van Vlierberghe, W. Verstraete, N. De Belie, Application of hydrogel encapsulated carbonate precipitating bacteria for approaching a realistic self-healing in concrete, Constr. Build. Mater. 68 (2014) 110–119.
[30] D. Homma, H. Mihashi, T. Nishiwaki, Self-healing capability of fibre reinforced cementitious composites, J. Adv. Concr. Technol. 7 (2009) 217–228.
[31] D. Snoeck, N. De Belie, Mechanical and self-healing properties of cementitious composites reinforced with flax and cottonised flax, and compared with polyvinyl alcohol fibres, Biosyst. Eng. 111 (2012) 325–335.
[32] Y. Yang, M.D. Lepech, E.H. Yang, V.C. Li, Autogenous healing of engineered cementitious composites under wet-dry cycles, Cem. Concr. Res. 39 (2009) 382–390.
[33] V.C. Li, Y.M. Lim, Y.-W. Chan, Feasibility study of a passive smart self - healing cementitious composite 8368 (1998) 819–827.
[34] M. Şahmaran, V.C. Li, Durability properties of micro-cracked ECC containing high volumes fly ash, Cem. Concr. Res. 39 (2009) 1033–1043.
[35] Y. Yang, E.H. Yang, V.C. Li, Autogenous healing of engineered cementitious composites at early age, Cem. Concr. Res. 41 (2011) 176–183.
[36] K. Van Tittelboom, J. Wang, M. Araújo, D. Snoeck, E. Gruyaert, B. Debbaut, H. Derluyn, V. Cnudde, E. Tsangouri, D. Van Hemelrijck, N. De Belie, Comparison of different approaches for self-healing concrete in a large-scale lab test, Constr. Build. Mater. 107 (2016) 125–137.
[37] D. Snoeck, K. Van Tittelboom, S. Steuperaert, P. Dubruel, N. De Belie, Self-healing cementitious materials by the combination of microfibres and superabsorbent polymers, J. Intell. Mater. Syst. Struct. 25 (2014) 13–24.
[38] E. Yang, Designing Added Functions in Engineered Cementitious Composites, (2008) 276.
[39] K. Sisomphon, O. Copuroglu, E.A.B. Koenders, Cement & Concrete composites self-healing of surface cracks in mortars with expansive additive and crystalline additive, Cem. Concr. Compos. 34 (2012) 566–574.
[40] S.Z. Qian, J. Zhou, E. Schlangen, Influence of curing condition and precracking time on the self-healing behavior of Engineered Cementitious Composites, Cem. Concr. Compos. 32 (2010) 686–693.
[41] A.E.M. Abd-Elmoaty, Self-healing of polymer modified concrete, Alexandria Eng. J. 50 (2011) 171–178.
[42] Y. Ohama, Recent progress in concrete-polymer composites, Adv. Cem. Based Mater. 5 (1997) 31–40.
[43] M.S.S. Zabanoot, Review of autogenous and autonomous self-healing concrete technologies for marine environments, WIT Trans. Built Environ. 196 (2020) 31–38.
[44] H.W. Kua, S. Gupta, A.N. Aday, W.V. Srubar, Biochar-immobilized bacteria and superabsorbent polymers enable self-healing of fiber-reinforced concrete after multiple damage cycles, Cem. Concr. Compos. 100 (2019) 35–52.
[45] R.A. Khushnood, Z.A. Qureshi, N. Shaheen, S. Ali, Bio-mineralized self-healing recycled aggregate concrete for sustainable infrastructure, Sci. Total Environ. 703 (2020), 135007.
[46] S. Guo S. Chidiac SELF-HEALING CONCRETE : A CRITICAL REVIEW 2019 1 10.
[47] X.F. Wang, Z.H. Yang, C. Fang, N.X. Han, G.M. Zhu, J.N. Tang, F. Xing, Evaluation of the mechanical performance recovery of self-healing cementitious materials – its methods and future development: A review, Constr. Build. Mater. 212 (2019) 400–421.
[48] J.A. Rosewitz, S. Wang, S.F. Scarlata, N. Rahbar, An enzymatic self-healing cementitious material, Appl. Mater. Today. 23 (2021), 101035.
[49] A.A. Griño, M.K.M. Daly, J.M.C. Ongpeng, Bio-influenced self-healing mechanism in concrete and its testing: A review, Appl. Sci. 10 (2020).
[50] W. Khaliq, M.B. Ehsan, Crack healing in concrete using various bio influenced self-healing techniques, Constr. Build. Mater. 102 (2016) 349–357.
[51] M. Sarkar, T. Chowdhury, B. Chattopadhyay, R. Gachhui, S. Mandal, Autonomous bioremediation of a microbial protein (bioremediase) in Pozzolana cementitious composite, J. Mater. Sci. 49 (2014) 4461–4468.
[52] A. Dakhane, S. Das, H. Hansen, S. O'Donnell, F. Hanoon, A. Rushton, C. Perla, N. Neithalath, Crack healing in cementitious mortars using enzyme-induced carbonate precipitation: Quantification based on fracture response, J. Mater. Civ. Eng. 30 (2018).
[53] E. Boquet, A. Boronat, A. Ramos-Cormenzana, Production of calcite (Calcium carbonate) crystals by soil bacteria is a general phenomenon, Nature. 246 (1973) 527–529.
[54] I. Ahenkorah, M.M. Rahman, M.R. Karim, P.R. Teasdale, A comparison of mechanical responses for microbial-and enzyme-induced cemented sand, Geotech. Lett. 10 (2020) 559–567.
[55] A. Almajed, Enzyme induced carbonate precipitation (EICP) for soil improvement, Dr. Deseration. 4 (2017) 9–15.
[56] A.J. of S. Nasser M. Hamdan, Applications of enzyme induced carbonate precipitation (EICP) for soil improvement J. Chem. Inf. Model. 53 2019 1689 1699.
[57] D. Ran, S. Kawasaki, Effective use of plant-derived urease in the field of geoenvironmental/ geotechnical engineering, J. Civ. Environ. Eng. 06 (2016) 1–13.
[58] D. Neupane, A.M. Asce, H. Yasuhara, N. Kinoshita, T. Unno, Applicability of Enzymatic Calcium Carbonate Precipitation as a Soil-Strengthening Technique 139 (2013) 2201–2211.
[59] P.J.V. Oliveira, L.D. Freitas, J.P.S.F. Carmona, Effect of Soil Type on the Enzymatic Calcium Carbonate Precipitation Process Used for Soil Improvement 29 (2017) 1–7.
[60] J.P.S.F. Carmona, P.J.V. Oliveira, Improvement of a sandy soil by enzymatic calcium carbonate precipitation 171 (2018).
[61] A. Almajed, H.K. Tirkolaei, E. Kavazanjian, Baseline investigation on enzyme-induced calcium carbonate precipitation, J. Geotech. Geoenvironmental Eng. 144 (2018) 1–11.
[62] I. Ahenkorah, M.M. Rahman, M.R. Karim, S. Beecham, Optimisation of chemical constituents on enzyme-induced carbonate precipitation in test-tube and soil, Geotech. Res. 8 (2021) 66–84.
[63] J. Larsen, M. Poulsen, T. Lundgaard, M. Agerbæk, Plugging of fractures in chalk reservoirs by enzyme-induced calcium carbonate precipitation, SPE Prod. Oper. 23 (2008) 478–783.
[64] M.J. Buehler, T. Ackbarow, Fracture mechanics of protein materials, Mater. Today. 10 (2007) 46–58.
[65] I.M. Weiss, S. Kaufmann, K. Mann, M. Fritz, Purification and characterization of perlucin and perlustrin, two new proteins from the shell of the mollusc haliotis laevigata, Biochem. Biophys. Res. Commun. 267 (2000) 17–21.
[66] K. Shimizu, J. Cha, G.D. Stucky, D.E. Morse, Silicatein : Cathepsin L-like protein in sponge biosilica, 1998. www.pnas.org.
[67] A. Chambers, C. Park, R.T. K Baker, N.M. Rodriguez, N. Kröger, R. Deutzmann, M. Sumper, Polycationic Peptides from Diatom Biosilica That Direct Silica Nanosphere Formation, 1997. http://science.sciencemag.org/ (accessed October 10, 2020).
[68] S. Sudo, T. Fujikawa, T. Nagakura, T. Ohkubo, K. Sakaguchi, M. Tanaka, K. Nakashima, T. Takahashi, Structures of mollusc shell framework proteins [6], Nature. 387 (1997) 563–564.
[69] H. Inoue, N. Ozaki, H. Nagasawa, Purification and structural determination of a phosphorylated peptide with anti-calcification and chitin-binding activities in the exoskeleton of the crayfish, Procambarus clarkii, Biosci. Biotechnol. Biochem. 65 (2001) 1840–1848.
[70] R. Lakshminarayanan, R.M. Kini, S. Valiyaveettil, Investigation of the role of ansocalcin in the biomineralization in goose eggshell matrix, n.d. www.pnas.orgcgidoi10.1073pnas.072658899 (accessed October 10, 2020).
[71] X. Xu, H. Guo, M. Li, H. Fu, Improving microbially induced calcium carbonate precipitation effects by nacre extractions, Geotech. Lett. 12 (2022) 1–7.
[72] A. Almajed, H.K. Tirkolaei, E. Kavazanjian, N. Hamdan, Enzyme induced biocementated sand with high strength at low carbonate content, Sci. Rep. 9 (2019) 1–7.
[73] R.A. Zulfikar, H. Putra, H. Yasuhara, Utilization of soybean as catalyst material in enzyme-mediated calcite precipitation (EMCP) for crack healing concrete, J. Civ. Eng. Forum. 1000 (2020) 59–70.
[74] Z.M. Ihsani, H. Putra, The utilization of milk as a catalyst material in enzyme-mediated calcite precipitation (EMCP) for crack-healing in concrete the utilization of milk as a catalyst material in enzyme-mediated calcite precipitation (EMCP) for crack-healing in concrete, Civ. Eng. Dimens. 23 (2021) 54–61.
[75] M. Nemati, G. Voordouw, Modification of porous media permeability, using calcium carbonate produced enzymatically in situ, Enzyme Microb. Technol. 33 (2003) 635–642.
[76] H. Bisswanger, Enzyme assays, Perspect. Sci. 1 (2014) 41–55.
[77] Y. Cao, Y.L. Xiong, Y. Cao, A.D. True, Food Hydrocolloids Interfacial properties of whey protein foams as in fl uenced by preheating and phenolic binding at neutral pH, Food Hydrocoll. 82 (2018) 379–387.
[78] S.M. Song, I.H. Kim, Biomineralization of calcium carbonate by adding aspartic acid and lysozyme 28 (2011) 1749–1753.
[79] I. Polowczyk, A. Bastrzyk, M. Fiedot, Protein-mediated precipitation of calcium carbonate, Materials (Basel). 9 (2016) 1–16.
[80] S. Savadkoohi, S. Kasapis, High pressure effects on the structural functionality of condensed globular-protein matrices, Int. J. Biol. Macromol. 88 (2016) 433–442.
[81] D. Barbano, Milk Protein Products - What Are They and What Role Do They Play in Lactose Reduced (Low " Carb ") Foods ? Low " Carb " Dairy Foods and Ingredients, in: Are Milk Protein Products Safe ? Milk components and separation processes, 2009, pp. 1–5.
[82] T.V. Arriaga, Controlled and tailored denaturation and aggregation of whey proteins Tatiana Vieira Arriaga Engenharia Biológica Júri, Thesis. (2011).
[83] M.H. Abd El-Salam, S. El-Shibiny, Natural biopolymers as nanocarriers for bioactive ingredients used in food industries, Elsevier Inc., 2016.
[84] N.S. Utay, D.M. Asmuth, S. Gharakhanian, M. Contreras, C.D. Warner, C.J. Detzel, Potential use of serum-derived bovine immunoglobulin/protein isolate for the management of COVID-19, Drug Dev. Res. 1–7 (2021).
[85] J.P.S.F. Carmona, P.J. Venda Oliveira, L.J.L. Lemos, A.M.G. Pedro, Improvement of a sandy soil by enzymatic calcium carbonate precipitation, (n.d.).
[86] C.T. Lim, F. Lolli, J.D. Thomas, B. Kola, M. Korbonits, Measurement of AMP-activated protein kinase activity and expression in response to ghrelin, Methods Enzymol. 514 (2012) 271–287.
[87] P.K. Smith, R.I. Krohn, G.T. Hermanson, A.K. Mallia, F.H. Gartner, M. D. Provenzano, E.K. Fujimoto, N.M. Goeke, B.J. Olson, D.C. Klenk, Measurement of protein using bicinchoninic acid, Anal. Biochem. 150 (1985) 76–85.
[88] S.D. Wu, H. Zhang, X.D. Dong, C.Y. Ning, A.S.L. Fok, Y. Wang, Physicochemical properties and in vitro cytocompatibility of modified titanium surfaces prepared via micro-arc oxidation with different calcium concentrations, Appl. Surf. Sci. 329 (2015) 347–355.
[89] K.M. Tang, W.S. Zhang, Y. Liu, W.Q. Zhu, J. Qiu, Physicochemical properties and in vitro osteocompatibility of different titanium surfaces stored in a saline solution, Mater. Res. Express. 8 (2021).
[90] L. Addadi, S. Weiner, Interactions between acidic proteins and crystals: Stereochemical requirements in biomineralization, Proc. Natl. Acad. Sci. U. S. A. 82 (1985) 4110–4114.

[91] D.M.E. Szebenyi, K. Moffat, The refined structure of vitamin D-dependent calcium-binding protein from bovine intestine. Molecular details, ion binding, and implications for the structure of other calcium-binding proteins, J. Biol. Chem. 261 (1986) 8761–8777.
[92] H. Xiao, L. Huang, W. Zhang, Z. Yin, Damage of proteins at the air/water interface: Surface tension characterizes globulin interface stability, Int. J. Pharm. 584 (2020), 119445.
[93] Z. Qiao, Z. Wang, C. Zhang, S. Yuan, Y. Zhu, J. Wang, PVAm–PIP/PS composite membrane with high performance for CO_2/N_2 separation, AIChE J. 59 (2012) 215–228.
[94] R. Luo, D. Zhang, Z. Zeng, R.L. Lytton, Effect of surface tension on the measurement of surface energy components of asphalt binders using the Wilhelmy Plate Method, Constr. Build. Mater. 98 (2015) 900–909.
[95] I. Ahenkorah, M.M. Rahman, M.R. Karim, P.R. Teasdale, Optimization of Enzyme Induced Carbonate Precipitation (EICP) as a Ground Improvement Technique, Geo-Congress 2020 Found. Soil Improv. Eros. (Hamblet. JP, Makhnenko R Budge AS (Eds)). Am. Soc. Civ. Eng. Reston, VA, USA. (2020) 552–561.
[96] P.Y. Loh, P. Shafigh, H.Y.B. Katman, Z. Ibrahim, S. Yousuf, Ph measurement of cement-based materials: The effect of particle size, Appl. Sci. 11 (2021).
[97] X.M. Wan, F.H. Wittmann, T.J. Zhao, H. Fan, Chloride content and pH value in the pore solution of concrete under carbonation, J. Zhejiang Univ. Sci. A. 14 (2013) 71–78.
[98] M.H. Derkani, A.J. Fletcher, M. Fedorov, W. Abdallah, B. Sauerer, J. Anderson, Z. J. Zhang, Mechanisms of surface charge modification of carbonates in aqueous electrolyte solutions, Colloids and Interfaces. 3 (2019).
[99] A.S. Dukhin, P.J. Goetz, Characterization of aggregation phenomena by means of acoustic and electroacoustic spectroscopy, Colloids Surfaces A Physicochem. Eng. Asp. 144 (1998) 49–58.
[100] Z.H. Xue, S.X. Dai, B. Bin Hu, Z.L. Du, Effect of Langmuir monolayer of bovine serum albumin protein on the morphology of calcium carbonate, Mater. Sci. Eng. C. 29 (2009) 1998–2002.
[101] H. Bian, Colloidal behavior of casein biopolymer in alkaline solution and its application in self-levelling underlayments (SLUs), (2012).
[102] A. Steudle, J. Pleiss, Modelling of lysozyme binding to a cation exchange surface at atomic detail: The role of flexibility, Biophys. J. 100 (2011) 3016–3024.
[103] P. Novák, V. Havlíček, Protein Extraction and Precipitation, Proteomic Profiling Anal, Chem. Crossroads Second Ed. (2016) 52–62.
[104] A.C. Dumetz, A.M. Chockla, E.W. Kaler, A.M. Lenhoff, Effects of pH on protein-protein interactions and implications for protein phase behavior, Biochim. Biophys. Acta - Proteins, Proteomics. 1784 (2008) 600–610.
[105] B.Y. Qin, M.C. Bewley, L.K. Creamer, H.M. Baker, E.N. Baker, G.B. Jameson, Structural basis of the tanford transition of bovine β-lactoglobulin, Biochemistry. 37 (1998) 14014–14023.
[106] J. Plank, H. Bian, Method to assess the quality of casein used as superplasticizer in self-levelling compounds, Cem. Concr. Res. 40 (2010) 710–715.
[107] D.H.G. Pelegrine, C.A. Gasparetto, Whey proteins solubility as function of temperature and pH, LWT - Food Sci. Technol. 38 (2005) 77–80.
[108] J. Li, C. Wang, X. Li, Y. Su, Y. Yang, X. Yu, Effects of pH and NaCl on the physicochemical and interfacial properties of egg white/yolk, Food Biosci. 23 (2018) 115–120.
[109] M. Boulet, M. Britten, F. Lamarche, Voluminosity of some food proteins in aqueous dispersions at various pH and ionic strengths, Food Hydrocoll. 12 (1998) 433–441.
[110] J. Plank, C. Winter, Competitive adsorption between superplasticizer and retarder molecules on mineral binder surface, Cem. Concr. Res. 38 (2008) 599–605.
[111] P.E. Stutzman, Scanning electron microscopy in concrete petrography, Mater. Sci. Concr. Spec. (2001) 59–72. http://fire.nist.gov/bfrlpubs/build01/PDF/b01086.pdf.
[112] L.S. Dent Glasser, E.E. Lachowski, K. Mohan, H.F.W. Taylor, A multi-method study of C3S hydration, Cem. Concr. Res. 8 (1978) 733–739.
[113] A. Zingg, F. Winnefeld, L. Holzer, J. Pakusch, S. Becker, L. Gauckler, Adsorption of polyelectrolytes and its influence on the rheology, zeta potential, and microstructure of various cement and hydrate phases, J. Colloid Interface Sci. 323 (2008) 301–312.
[114] B. Njegić-Džakula, G. Falini, L. Brečević, Ž. Skoko, D. Kralj, Effects of initial supersaturation on spontaneous precipitation of calcium carbonate in the presence of charged poly-l-amino acids, J. Colloid Interface Sci. 343 (2010) 553–563.
[115] V. Pipich, M. Balz, S.E. Wolf, W. Tremel, D. Schwann, Nucleation and growth of CaCO3 mediated by the egg-white protein ovalbumin: A time-resolved in situ study using small-angle neutron scattering, J. Am. Chem. Soc. 130 (2008) 6879–6892.
[116] T.L. Hughes, C.M. Methven, T.G.J. Jones, S.E. Pelham, P. Fletcher, C. Hall, Determining cement composition by Fourier transform infrared spectroscopy, Adv. Cem. Based Mater. 2 (1995) 91–104.
[117] R. Ylmén, U. Jäglid, B.M. Steenari, I. Panas, Early hydration and setting of Portland cement monitored by IR, SEM and Vicat techniques, Cem. Concr. Res. 39 (2009) 433–439.
[118] J.E. Kinsella, Functional properties of proteins: Possible relationships between structure and function in foams, Food Chem. 7 (1981) 273–288.
[119] F. Zhan, J. Hu, C. He, J. Sun, J. Li, B. Li, Complexation between sodium caseinate and gallic acid: Effects on foam properties and interfacial properties of foam, Food Hydrocoll. 99 (2020), 105365.
[120] C. Valenzuela, L. Abugoch, C. Tapia, A. Gamboa, Effect of alkaline extraction on the structure of the protein of quinoa (Chenopodium quinoa Willd.) and its influence on film formation, Int. J. Food Sci. Technol. 48 (2013) 843–849.
[121] L. Yang, L. She, J. Zhou, Y. Cao, X. Ma, Interaction of lysozyme during calcium carbonate precipitation at supramolecular level 9 (2006) 164–166.
[122] M.Y.A. Mollah, W. Yu, R. Schennach, D.L. Cocke, Fourier transform infrared spectroscopic investigation of the early hydration of Portland cement and the influence of sodium lignosulfonate, Cem. Concr. Res. 30 (2000) 267–273.
[123] H. Tong, W. Ma, L. Wang, P. Wan, J. Hu, L. Cao, Control over the crystal phase, shape, size and aggregation of calcium carbonate via a L-aspartic acid inducing process, Biomaterials. 25 (2004) 3923–3929.
[124] L. Štajner, J. Kontrec, B. Njegić Džakula, N. Maltar-Strmečki, M. Plodinec, D. M. Lyons, D. Kralj, The effect of different amino acids on spontaneous precipitation of calcium carbonate polymorphs, J. Cryst. Growth. 486 (2018) 71–81.
[125] R.S. Lin, X.Y. Wang, H.S. Lee, H.K. Cho, Hydration and microstructure of cement pastes with calcined Hwangtoh Clay, Materials (Basel). 12 (2019) 1–19.
[126] E. Qoku, T.A. Bier, T. Westphal, Phase assemblage in ettringite-forming cement pastes: A X-ray diffraction and thermal analysis characterization, J. Build. Eng. 12 (2017) 37–50.
[127] B. Lothenbach, G. Le Saout, M. Ben Haha, R. Figi, E. Wieland, Hydration of a low-alkali CEM III/B-SiO 2 cement (LAC), Cem. Concr. Res. 42 (2012) 410–423.
[128] G. Ye, X. Liu, G. De Schutter, A.M. Poppe, L. Taerwe, Influence of limestone powder used as filler in SCC on hydration and microstructure of cement pastes, Cem. Concr. Compos. 29 (2007) 94–102.
[129] L.P. Esteves, On the hydration of water-entrained cement-silica systems: Combined SEM, XRD and thermal analysis in cement pastes, Thermochim. Acta. 518 (2011) 27–35.
[130] I. Pane, W. Hansen, Investigation of blended cement hydration by isothermal calorimetry and thermal analysis, Cem. Concr. Res. 35 (2005) 1155–1164.
[131] A. Hernández-Hernández, A.B. Rodríguez-Navarro, J. Gómez-Morales, C. Jiménez-Lopez, Y. Nys, J.M. García-Ruiz, Influence of Model Globular Proteins with Different Isoelectric & DESIGN 2008, Cryst. Growth Des. 8 (2008) 1495–1502.
[132] H. Khodadadi Tirkolaei, N. Javadi, V. Krishnan, N. Hamdan, E. Kavazanjian, Crude urease extract for biocementation, J. Mater. Civ. Eng. 32 (2020) 04020374.
[133] K. Martin, H.K. Tirkolaei, E. Kavazanjian, Enhancing the strength of granular material with a modified enzyme-induced carbonate precipitation (EICP) treatment solution, Constr. Build. Mater. 271 (2021), 121529.
[134] J.F. Schmitz, Enzyme modified soy flour adhesives, (2009).
[135] M.J. Brennan, S.E. Hollingshead, J.J. Wilker, J.C. Liu, Critical factors for the bulk adhesion of engineered elastomeric proteins, R. Soc. Open Sci. 5 (2018).
[136] W. Huang, X. Sun, Adhesive properties of soy proteins modified by urea and guanidine hydrochloride, JAOCS, J. Am. Oil Chem. Soc. 77 (2000) 101–104.
[137] Y. Liu, K. Li, Development and characterization of adhesives from soy protein for bonding wood, Int. J. Adhes. Adhes. 27 (2007) 59–67.
[138] B. Cantaert, D. Kuo, S. Matsumura, T. Nishimura, T. Sakamoto, T. Kato, Use of amorphous calcium carbonate for the design of new materials, Chempluschem. 82 (2017) 107–120.
[139] G. Mayer, Rigid biological systems as models for synthetic composites, Science (80-,) 310 (2005) 1144–1147.
[140] S. Chandra, J. Aavik, Influence of black gram (natural organic material) addition as admixture in cement mortar and concrete, Cem. Concr. Res. 13 (1983) 423–430.
[141] B. Liu, J. Shi, M. Sun, Z. He, H. Xu, J. Tan, Mechanical and permeability properties of polymer-modified concrete using hydrophobic agent, J. Build. Eng. 31 (2020), 101337.
[142] L. Courard, Z. Zhao, F. Michel, Influence of hydrophobic product nature and concentration on carbonation resistance of cultural heritage concrete buildings, Cem. Concr. Compos. 115 (2021) 1–11.
[143] S. Weisheit, S.H. Unterberger, T. Bader, R. Lackner, Assessment of test methods for characterizing the hydrophobic nature of surface-treated High performance concrete, Constr. Build. Mater. 110 (2016) 145–153.